Cell Metabolism
Article

Macrophage-Derived AIM Is Endocytosed into Adipocytes and Decreases Lipid Droplets via Inhibition of Fatty Acid Synthase Activity

Jun Kurokawa,[1] Satoko Arai,[1] Katsuhiko Nakashima,[1] Hiromichi Nagano,[1] Akemi Nishijima,[1] Keishi Miyata,[3] Rui Ose,[4] Mayumi Mori,[1] Naoto Kubota,[2] Takashi Kadowaki,[2] Yuichi Oike,[3] Hisashi Koga,[4] Maria Febbraio,[5] Toshihiko Iwanaga,[6] and Toru Miyazaki[1,*]

[1]Laboratory of Molecular Biomedicine for Pathogenesis, Center for Disease Biology and Integrative Medicine, Faculty of Medicine
[2]Department of Internal Medicine, Graduate School of Medicine
The University of Tokyo, Tokyo, 113-0033, Japan
[3]Department of Molecular Genetics, Graduate School of Medical Sciences, Kumamoto University, Kumamoto, 860-8556, Japan
[4]Department of Human Genome Research, Kazusa DNA Research Institute, Kisarazu, Chiba, 292-0818, Japan
[5]Department of Cell Biology, Lerner Research Institute, Cleveland Clinic Foundation, Cleveland, OH 44195, USA
[6]Department of Functional Morphology, Laboratory of Histology and Cytology, Hokkaido University Graduate School of Medicine, Sapporo, Hokkaido, 060-0815, Japan
*Correspondence: tm@m.u-tokyo.ac.jp
DOI 10.1016/j.cmet.2010.04.013

SUMMARY

Macrophages infiltrate adipose tissue in obesity and are involved in the induction of inflammation, thereby contributing to the development of obesity-associated metabolic disorders. Here, we show that the macrophage-derived soluble protein AIM is endocytosed into adipocytes via CD36. Within adipocytes, AIM associates with cytosolic fatty acid synthase (FAS), thereby decreasing FAS activity. This decreases lipid droplet size, stimulating the efflux of free fatty acids and glycerol from adipocytes. As an additional consequence of FAS inhibition, AIM prevents preadipocyte maturation. In vivo, the increase in adipocyte size and fat weight induced by high-fat diet (HFD) was accelerated in *AIM*-deficient ($AIM^{-/-}$) mice compared to $AIM^{+/+}$ mice. Moreover, injection of recombinant AIM in $AIM^{-/-}$ mice suppresses the increase in fat mass induced by HFD. Interestingly, metabolic rates are comparable in $AIM^{-/-}$ and $AIM^{+/+}$ mice, suggesting that AIM specifically influences adipocyte status. Thus, this AIM function in adipocytes may be physiologically relevant to obesity progression.

INTRODUCTION

It is well known that adipose tissues in obesity are in a state of chronic inflammation (Olshansky et al., 2005; Baker et al., 2007). Accumulating evidence indicates that this inflammation is induced predominantly by the recruitment of a large number of macrophages into adipose tissues (Olshansky et al., 2005; Baker et al., 2007; Apovian et al., 2008). Although the precise mechanism underlying the initiation of macrophage recruitment to adipose tissues remains a matter of debate, adipose tissue macrophage number rapidly increases as obesity progresses (Surmi and Hasty, 2008). The subclinical inflammatory state of adipose tissues is tightly associated with insulin resistance of adipose tissues as well as systemic insulin resistance and cardiovascular disease (Neels and Olefsky, 2006; Shoelson et al., 2006). Thus, adipose tissue macrophages are thought to play key roles in several obesity-induced metabolic disorders. However, whether adipose tissue macrophages also exert direct effect(s) on surrounding adipocytes, independent of inflammatory responses, remains to be determined. To address this question, we focused on the protein AIM (apoptosis inhibitor of macrophage, also known Spα, Api6, and CD5L) in the context of its effects on adipocytes, because AIM is produced and secreted specifically by tissue macrophages, and its expression in vivo is markedly increased with obesity progression in mice (Miyazaki et al., 1999; Arai et al., 2005).

The AIM protein is a member of the scavenger receptor cysteine-rich superfamily (SRCR-SF) and was initially identified as an apoptosis inhibitor that supports the survival of macrophages themselves against various apoptosis-inducing stimuli (Miyazaki et al., 1999). As a secreted molecule, AIM has been detected in human and mouse blood at varying levels (Miyazaki et al., 1999; Gebe et al., 1997, 2000; Gangadharan et al., 2007; Kim et al., 2008; Gray et al., 2009). Based on the observation that *AIM* is a direct target for regulation by nuclear receptor LXR/RXR heterodimers (Joseph et al., 2004; Valledor et al., 2004), we found that AIM is expressed in lipid-laden macrophages at atherosclerotic lesions, and this induction is associated with atherosclerogenesis by supporting the survival of macrophages within lesions (Arai et al., 2005). Other studies have shown that AIM appears to be multifunctional and is effective in cell types other than macrophages, including B and natural killer (NK) T lymphocytes (Yusa et al., 1999; Kuwata et al., 2003) and myeloid cells (Qu et al., 2009). However, the functional nature of AIM remains enigmatic because we are ignorant of the precise mechanism by which it elicits its effects.

In the present study, we assessed the expression of AIM by adipose tissue macrophages in obese mice. We also analyzed how AIM interacts with adipocytes. In addition, an effect of AIM on adipocytes and its consequence with respect to the regulation of adipocyte size in vivo was determined. Finally, we investigated the molecular mechanism underlying this role of AIM in adipocytes. Based on these results, we will discuss the putative role of AIM on the state of adipose tissues.

RESULTS

AIM in Adipose Tissue Macrophages in Obese Mice

We first assessed the expression of AIM by adipose tissue macrophages in obese C57BL/6 (B6) mice after the administration of a high-fat diet (HFD) (fat kcal 60%) for 20 weeks. In obese mice, large numbers of macrophages were observed within visceral fat tissues, forming clusters or crown-like structures (CLSs) (Cinti et al., 2005), whereas few adipose tissue macrophages were detected in lean mice (Figure 1A). As shown in Figure 1B, macrophages (stained with F4/80 pan macrophage antibody) in obese adipose tissues showed staining with an antibody specific to AIM (SA-1) (Arai et al., 2005). These AIM-positive macrophages were also positive for interleukin (IL)-6 staining, indicating that they were the inflammatory macrophage type (M1) (Figure 1B). In contrast, F4/80-positive macrophages within adipose tissues from lean mice were negative for AIM and IL-6 staining (Figure 1B). Similarly, the serum level of AIM was increased in obese mice compared to lean mice (Figure 1C). It is possible that AIM detectable in lean mice is derived predominantly from macrophages in other macrophage-containing tissues (Miyazaki et al., 1999; Gebe et al., 2000; Arai et al., 2005). To exclude the possible expression of AIM by adipocytes, adipocytes from epididymal fat tissue of obese mice were fractionated after collagenase treatment (Brake et al., 2006) and assessed for *AIM* expression by quantitative real-time PCR (QPCR). No *AIM* expression was observed in purified adipocytes (Figure S1A). In addition, 3T3-L1 adipocytes were analyzed after the induction of maturation by insulin, dexamethasone (DEX), and isobutylmethylxanthine (IBMX). Again, *AIM* expression was not detectable in mature 3T3-L1 adipocytes (Figure S1B).

Endocytosis of AIM into Adipocytes

Intriguingly, although we found no *AIM* expression by adipocytes (Figure S1), some adipocytes surrounding adipose tissue macrophages in obese mice showed AIM staining (Figure 2A, arrows). This may indicate a physiologic association of AIM with tissue adipocytes. To test this possibility, we injected recombinant AIM (rAIM) into epididymal fat in obese male $AIM^{-/-}$ mice and analyzed fat tissue histologically 3 hr later. Epididymal fat was selected for this experiment owing to its ease of manipulation. Interaction of AIM with adipocytes was clearly confirmed in $AIM^{-/-}$ mice. As shown in Figure 2B (left and middle lanes), $AIM^{-/-}$ adipocytes were positive for AIM staining when rAIM was injected locally into fat tissue (Figure 2B, left and middle lanes). Staining for AIM was also detected in adipocytes in fat tissue in which rAIM was administered systemically to $AIM^{-/-}$ mice via intravenous (i.v.) injection (Figure 2B, right lane). These results implicate adipocytes as a target cell type for AIM. Macrophages also stained for AIM in $AIM^{-/-}$ adipose tissue after injection of rAIM (Figure 2B), consistent with the fact that AIM is effective in macrophages (Miyazaki et al., 1999; Arai et al., 2005).

To further investigate how AIM interacts with adipocytes, differentiated 3T3-L1 adipocytes were treated with rAIM, and the association of rAIM with these cells was analyzed by confocal microscopy. Interestingly, rAIM accumulated within the cytoplasm of adipocytes, forming many dots within the intracellular compartment (Figure 3A). After stimulation with insulin, DEX, and IBMX, a large proportion of 3T3-L1 cells underwent differentiation, expressing peroxisome proliferator-activated receptor γ 2 (PPARγ2) at a high level, whereas some cells remained in an undifferentiated state, expressing PPARγ2 at a low or undetectable level (Madsen et al., 2003). As shown in Figure 3A, among this heterogeneous cell population, mature adipocytes strongly positive for PPARγ2 (yellow arrows) efficiently incorporated rAIM, whereas adipocytes faintly positive for PPARγ2 (blue arrows) or negative (white arrows) did not (left and middle lanes). Preadipocytes not stimulated by insulin, DEX, and IBMX did not incorporate rAIM (Figure 3A, right lane). As shown in Figure 3B, incorporated rAIM colocalized with early endosomes (positive for early endosome antigen 1; EEA1) but not with late endosomes (positive for Rab7) or recycling endosomes (positive for Rab11). These results suggest that incorporated AIM was transported to the cytosol during endosome maturation. No costaining for AIM and lysosomes or lipid droplets was observed (Figure 3B; AIM + lysosome, AIM + lipid droplets). Additional analysis of the cells by electron microscopy shown may support the specific colocalization of AIM with endosomes (Figures 3C and S2). Gold particles indicating rAIM immunoreactivity were mainly associated with endosome-like structures, where the limiting membrane of the structures and the periphery of their contents were heavily labeled (Figure 3C). Endocytosis of rAIM was observed at the cell membrane (Figure 3C, indicated by arrows). Other organelles were essentially negative for AIM immunolabeling (Figure S2). All these data suggest that AIM is incorporated into adipocytes via endocytosis, is transported to the cytoplasm, and function intracellularly.

Cell-Surface CD36-Mediated Internalization of AIM

The accumulation of AIM at the membrane of endosome-like particles (Figure 3C) indicates that the internalization of exogenous AIM may be mediated by a cell-surface molecule. As a candidate molecule responsible for endocytosis, we focused on scavenger receptor CD36 because it promotes the internalization of various molecules, including lipoproteins and fatty acids (Greenwalt et al., 1992; Ibrahimi and Abumrad, 2002), and it is expressed by adipocytes and macrophages, which are target cells for AIM. Thus, we assessed whether treatment of 3T3-L1 adipocytes with a neutralizing antibody against CD36 (clone JC63.1; mouse IgA) interfered with rAIM uptake. As shown in Figure 3D, incorporation of rAIM was drastically decreased in the presence of this neutralizing antibody. In addition, we injected rAIM intravenously into $CD36^{-/-}$ (Febbraio et al., 1999) and $CD36^{+/+}$ mice and analyzed the incorporation of rAIM into adipose tissues. As shown in Figure 3E, incorporation of rAIM into adipocytes was markedly less in $CD36^{-/-}$ mice compared to $CD36^{+/+}$ mice. These data strongly indicate that CD36 is responsible for AIM internalization. This was also supported by microscopic analysis of the association of rAIM

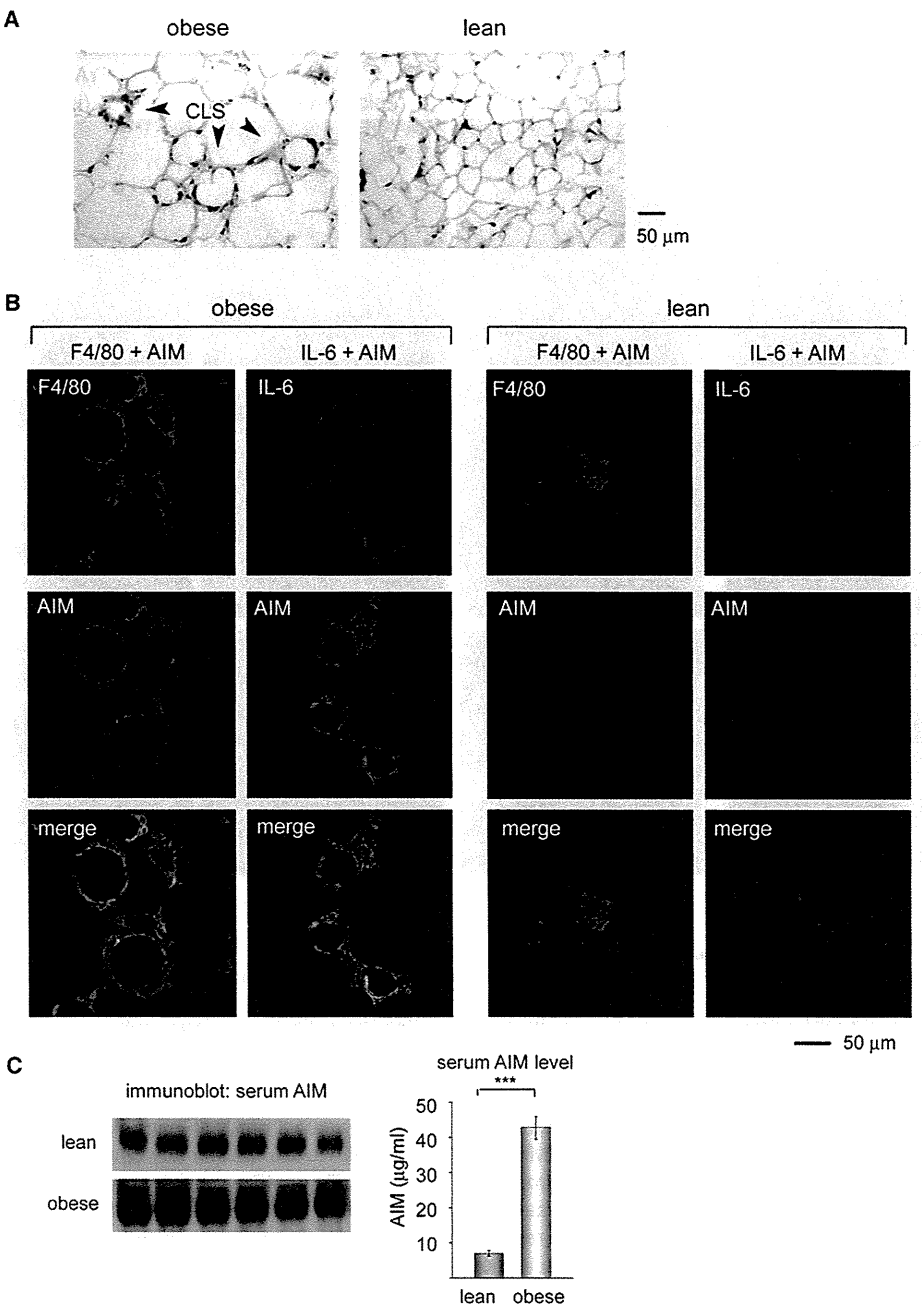

Figure 1. Immunohistochemical Analysis of AIM in Adipose Tissues

(A) Representative photomicrographs of visceral fat tissue from lean (fed with normal chow) or obese (fed with a HFD for 20 weeks) wild-type B6 mice stained with hematoxylin and eosin (H&E). The crown-like structures (CLSs) formed by recruited macrophages are indicated by arrows.

(B) Specimens of visceral fat tissues from lean or obese B6 mice were costained for AIM (green) and F4/80 (pan macrophage marker; red) or AIM (green) and IL-6 (red).

(C) Immunoblotting for serum AIM. A volume of 1 μl of serum from six separate lean (fed with normal chow) or obese (fed with a HFD for 20 weeks) mice was used. Results for immunoblots and actual AIM concentration are presented. AIM concentration was calculated by comparison with the density obtained with various amounts of recombinant AIM (rAIM) on the same blot. The density of the signal was calculated using image analysis software NIH ImageJ. Error bar indicates SEM.

with Flag-tagged mouse CD36 expressed on the surface of HEK293T cells. Notably, the accumulation of rAIM staining (green) was specifically colocalized with Flag-CD36 (red) on the cell surface (Figure S3).

AIM Decreases Adipocyte Lipid Droplet Size

We next assessed the effect of incorporated AIM in host adipocytes. To achieve this, differentiated 3T3-L1 adipocytes in culture (at 4 days after maturation stimulation) were challenged

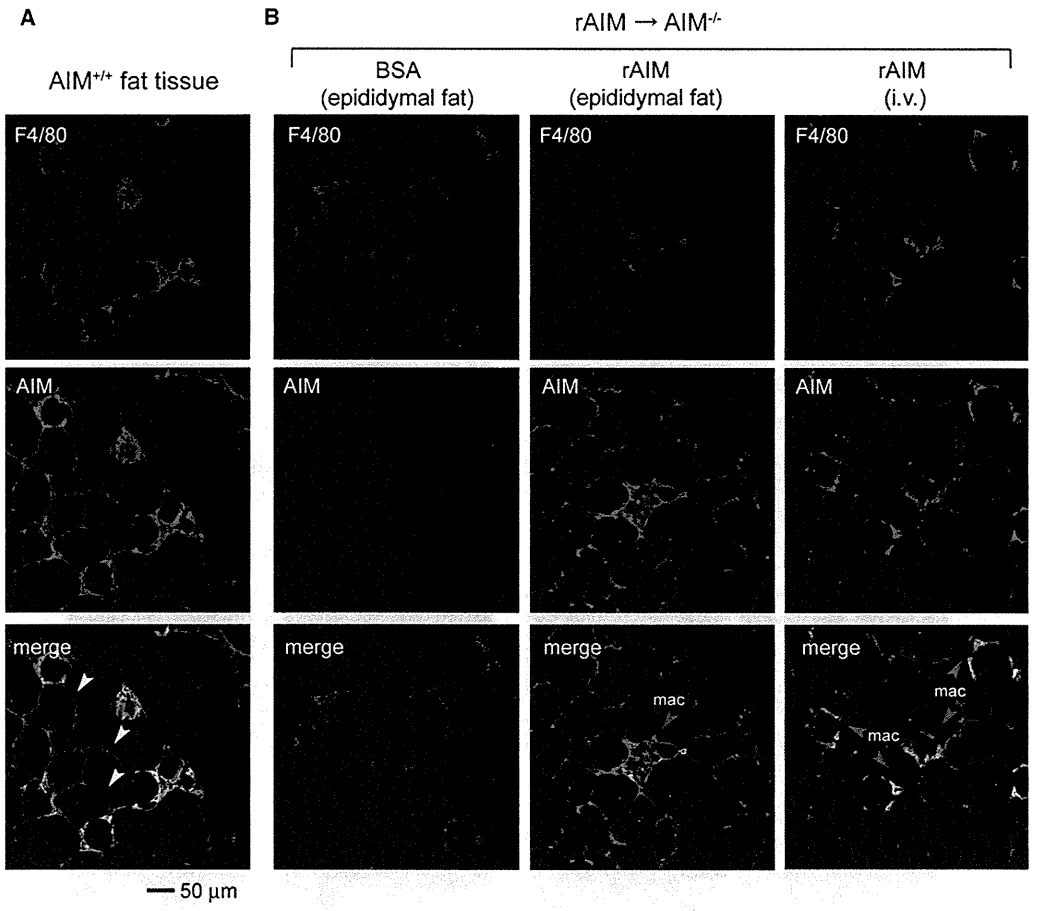

Figure 2. Association of Exogenous AIM with Adipocytes

(A) Epididymal fat sections were stained for AIM (green) and F4/80 (red). Staining for AIM was detected in macrophages and some adipocytes (arrows).

(B) Uptake of rAIM by *AIM*$^{-/-}$ adipocytes in vivo. *AIM*$^{-/-}$ mice were injected with rAIM (middle lane) or BSA (left lane) directly into the epididymal fat (total 100 μg for each at several loci) or with rAIM systemically (300 μg) via i.v. injection (right lane). Three hours after injection, tissue sections were generated and stained for AIM (green) and macrophage F4/80 (red). mac: macrophage.

with rAIM. Remarkably, the size of lipid droplets within the cells was decreased after a 6 day incubation of cells with rAIM (Figure 4A). In addition, the number of cells containing lipid droplets was also decreased (Figure 4A). Supernatant viscosity was also markedly enhanced by the administration of rAIM. These results suggest that rAIM induced a lipolytic response, resulting in the liberation of droplet components such as glycerol and fatty acids from the cells (Zechner et al., 2005; Duncan et al., 2007). We tested this possibility by determining the efflux of glycerol and free fatty acids (FFAs) on days 2, 4, and 6 after stimulation with rAIM. As shown in Figure 4B, the amount of glycerol and FFAs in the supernatant increased significantly when adipocytes were maintained in rAIM. In vivo, basal levels of FFA and glycerol in serum were lower in *AIM*$^{-/-}$ obese mice than in *AIM*$^{+/+}$ obese mice (Figure 4C), consistent with the in vitro results.

mRNA levels for *fat-specific protein 27* (*FSP27*, also termed *cidec*), *Perilipin*, and *Adipophilin*, important elements involved in the formation of lipid droplets (Ducharme and Bickel, 2008; Puri and Czech, 2008), were decreased after treatment of 3T3-L1 adipocytes with rAIM (Figure 4D). A significant decrease in these mRNA levels was already apparent 2 days after challenge with rAIM (Figure 4D), consistent with the progression of lipolysis, as reported previously (Zechner et al., 2005; Nishino et al., 2008). In contrast, mRNA level of mature adipocyte markers such as *PPARγ2*, *CCAAT-enhancer-binding protein α* (*C/EBPα*), and *glucose transporter 4* (*GLUT4*) and an immature adipocyte marker, *Preadipocyte factor-1* (*PREF-1*) (Smas and Sul, 1993), was not remarkably changed in response to rAIM treatment, suggesting that rAIM did not appear to induce dedifferentiation of adipocytes (Figure 4D). Local injection of rAIM into epididymal fat tissue of *AIM*$^{-/-}$ mice resulted in similar changes in mRNA levels of these genes (Figure 4E).

Increase in Adipocyte Size and Adipose Tissue Mass in *AIM*$^{-/-}$ Mice

Consistent with the observations in 3T3-L1 cells, the size of visceral fat adipocytes was larger in obese *AIM*$^{-/-}$ mice than in obese *AIM*$^{+/+}$ mice (Figure 5A). Relevant to this enlargement of

adipocytes, the increase in weight of both visceral and subcutaneous fat tissues in mice fed with a HFD (12 weeks) was more accelerated in $AIM^{-/-}$ mice than in $AIM^{+/+}$ mice (Figure 5B). This difference was also apparent in mice fed with a HFD for a longer period (20 weeks) (Figure S4). It is noteworthy that $AIM^{-/-}$ mice and $AIM^{+/+}$ mice fed with a HFD showed comparable metabolic rates (e.g., body temperature, oxygen consumption, and food intake) (Figure S5). Locomotor activity was also equivalent in both types of mice (Figure S5). Thus, AIM appears to influence adipose tissue mass by specifically affecting adipocytes.

We also injected rAIM intraperitoneally (twice a week) into $AIM^{-/-}$ mice fed with a HFD for 5 weeks to assess whether rAIM administration might suppress the increase in adipose tissue mass. As expected, the increase in weight of whole-body as well as both visceral and subcutaneous fat tissues was significantly less in mice injected with rAIM than in those injected with bovine serum albumin (BSA) (Figure 5C). As observed for the treatment of 3T3-L1 adipocytes with rAIM (Figure 4D), mRNA levels of *FSP27*, *Perilipin*, and *Adipophilin* were also lower in the epididymal adipose tissue in mice injected with rAIM (Figure 5D). Interestingly, mRNA level of *PREF-1* was higher in rAIM-injected mice, although that of *PPARγ2*, *C/EBPα*, or *GLUT4* was similar in mice injected with rAIM or BSA (Figure 5D).

AIM Decreased Fatty Acid Synthase Activity

We were interested in the intracellular target molecule(s) of incorporated AIM in adipocytes. To this end, we performed immunoprecipitation-mass spectrometry (IP-MS) analysis with lysates from different cells and tissues. Fatty acid synthase (FAS) was identified as a candidate molecule with the potential to associate with AIM (other proteins, including carbamoyl phosphate synthase-1, major vault protein, and aldehyde dehydrogenase 1 family member L1, were also associated with AIM; complete results of this analysis will be published elsewhere). FAS is highly expressed in adipose tissues and catalyzes the synthesis of saturated fatty acids, such as palmitate, from acetyl-CoA and malonyl-CoA precursors. Accumulating evidence has highlighted critical roles of FAS in a variety of biological aspects, including early embryogenesis (Chirala et al., 2003), in addition to providing a metabolic substrate. A number of biochemical and genetic studies have suggested the involvement of FAS in the regulation of adipose tissue mass (Loftus et al., 2000; Makimura et al., 2001; Kumar et al., 2002; Mobbs and Makimura, 2002; Shimokawa et al., 2002; Kovacs et al., 2004; Liu et al., 2004; Ronnett et al., 2005; Schmid et al., 2005; Chakravarthy et al., 2009a).

We confirmed the association of AIM and FAS in vivo and in vitro. After injecting rAIM into epididymal fat of obese $AIM^{-/-}$ mice, we precipitated incorporated rAIM from fat tissue lysates and addressed whether endogenous FAS was also precipitated. As shown in Figure 6A, the proteins coprecipitated, confirming the association of incorporated AIM and cytosolic FAS. In addition, a coimmunoprecipitation (coIP) assay with HEK293T cells expressing Flag-tagged FAS and HA-tagged AIM showed that the two proteins coprecipitated, indicating that AIM possesses the potential to bind to FAS (Figure 6B).

We also attempted to map FAS-binding region(s) for AIM. FAS consists of seven discrete functional domains: ketoacyl synthase (KS), malonyl/acetyl transferase (MAT), dehydrase (DH), enoylreductase (ER), ketoreductase (KR), acyl carrier protein (ACP), and thioesterase (TE) (Smith, 1994). There is a central core (CC) between the DH and ER domains that has no known catalytic function and may play a structural role in stabilizing the dimer (illustrated in schematic in Figure 6C). We assessed the association of HA-tagged AIM with each FAS region tagged with a Flag sequence by coIP assay. Notably, AIM bound specifically to ER, DH, TE, and CC domains, but not to the N-terminal region containing KS and MAT, which are involved in the initial acyl chain assembly (i.e., condensation of acetyl and malonyl moieties to 3-ketobutyryl-ACP along with the release of CO_2) (Figures 6C and S6). Thus, AIM appears to influence the elongation of fatty acid chains (which involves ER and DH) and the release of synthesized palmitate (which is dependent on TE).

The association of AIM with the CC domain suggested that AIM might also affect the dimerization of FAS. It is well known that FAS is highly functional as a dimerized form, whereas monomeric FAS possesses little or no activity (Smith et al., 1985; Asturias et al., 2005). Therefore, we analyzed the dimer/monomer status of FAS protein in 3T3-L1 adipocytes after culture in the presence or absence of rAIM for 6 days. As expected, the proportion of dimerized FAS (500 kDa) (as assessed by separation of FAS on a Tris-acetate gel specific for large molecular weight proteins) was significantly less in cells maintained in the presence of rAIM than in cells without rAIM treatment (Figure 6D).

Consistent with these results, the enzymatic activity of FAS (as assessed by the consumption of malonyl-CoA) (Kelley et al., 1986) was markedly decreased in 3T3-L1 adipocytes treated with rAIM as above (Figure 6E). The decrease in FAS activity induced by rAIM (5 μg/ml) was at a similar level to that induced by C75, a specific FAS inhibitor (Kuhajda et al., 2000), when used at a functional concentration (25 μM) (Figure 6E). In vivo, FAS activity was significantly increased in epididymal fat of $AIM^{-/-}$ mice compared to that of $AIM^{+/+}$ mice (Figure 6F). In addition, supplementation of rAIM via direct injection decreased FAS activity in epididymal fat of $AIM^{-/-}$ mice (Figure 6G).

AIM and FAS Inhibitor C75 Showed Comparable Effects on Adipocytes

To address whether the effect of AIM on adipocytes resulted from the suppression of FAS activity, we tested whether treatment of 3T3-L1 adipocytes with AIM or FAS inhibitor C75 had similar consequences. As expected, rAIM (5 μg/ml) and C75 (25 μM) induced an increase in the efflux of glycerol and FFAs at comparable levels (Figure 7A). We also assessed the influence of AIM on adipogenesis, because Schmid et al. (2005) reported that inhibition of FAS prevented preadipocyte differentiation. Interestingly, the presence of rAIM during stimulation by insulin, DEX, and IBMX (48 hr) completely prevented differentiation of 3T3-L1 preadipocytes toward mature adipocytes at a level equivalent to that observed with C75 (Figure 7B). The numbers of dead cells did not increase in the presence of rAIM at different time points, as assessed by staining with trypan blue or propidium iodide (data not shown). This excludes the argument that rAIM might induce death of 3T3-L1 cells, appearing to decrease the overall number of mature adipocytes. In addition, AIM did not simply attenuate either (or all) of the three stimulators via

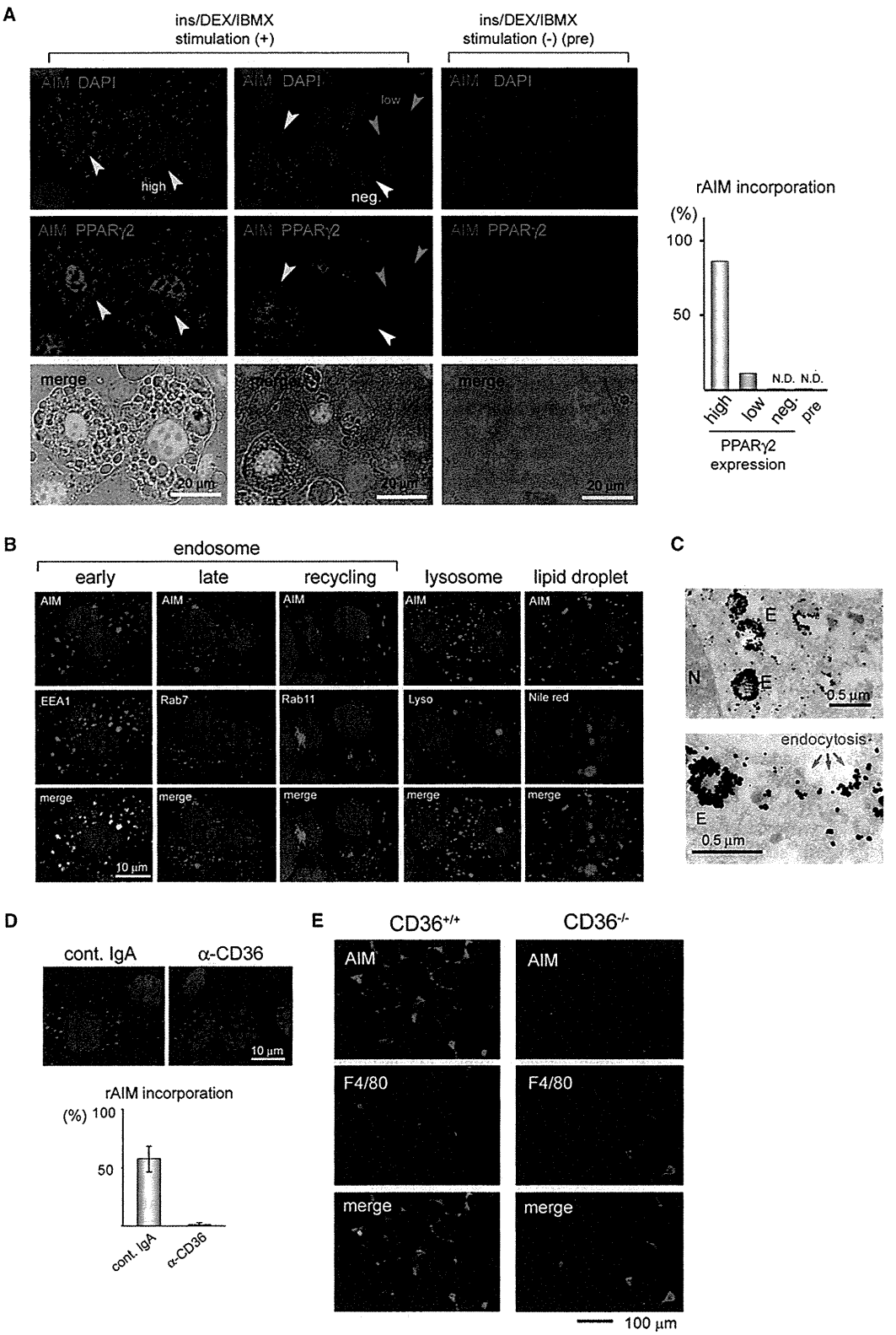
A
ins/DEX/IBMX stimulation (+)
ins/DEX/IBMX stimulation (-) (pre)
AIM DAPI
high
low
neg.
AIM PPARγ2
merge
20 μm
rAIM incorporation
(%)
100
50
N.D. N.D.
high
low
neg.
pre
PPARγ2 expression
B
endosome
early
late
recycling
lysosome
lipid droplet
AIM
EEA1
Rab7
Rab11
Lyso
Nile red
merge
10 μm
C
E
N
0.5 μm
endocytosis
D
cont. IgA
α-CD36
10 μm
rAIM incorporation
(%) 100
50
cont. IgA
α-CD36
E
CD36+/+
CD36-/-
AIM
F4/80
merge
100 μm

chemical interaction; coincubation with rAIM followed by removal of rAIM via column purification did not alter their ability to induce 3T3-L1 cell differentiation (Figure S7).

Consistent with these morphologic results, cells cultured in the presence of rAIM or C75 showed a marked decrease in mRNA levels of *C/EBPα* and *PPARγ* (*γ1* and *γ2*), the master regulator genes for adipogenesis (Rosen et al., 1999; Wu et al., 1999a; Farmer, 2006), as well as of downstream genes characteristic of functional adipocytes, such as *CD36* and *GLUT4*, compared to cells differentiated in the absence of rAIM or C75 (Figure 7C). Altogether, these results indicate that AIM affected adipocytes by inhibiting FAS activity.

Inhibition of FAS Did Not Activate cAMP-Dependent Lipolysis

During periods of energy deprivation, adipocytes undergo lipolysis via stimulation of a G protein-coupled receptor/cyclic AMP (cAMP)-dependent signaling cascade, followed by phosphorylation of protein kinase A (PKA), which activates hormone-sensitive lipase (HSL). At the same time, the level of *adipose triglyceride lipase* (*ATGL*) mRNA also increases (Wu et al., 1999b; He et al., 2003; Holm, 2003; Finn and Dice, 2006; Zechner et al., 2005; Duncan et al., 2007; Lafontan, 2008). Interestingly, however, despite the lipolytic consequences, treatment of 3T3-L1 adipocytes with rAIM or C75 did not upregulate the phosphorylation of PKA (Figure S8A). In addition, the levels of *ATGL* and *HSL* mRNA did not increase in response to AIM (Figure S8B). Thus, unlike in a starved situation, inhibition of FAS does not stimulate cAMP/PKA-dependent lipolysis. Note that the level of phosphorylation of 5′-AMP-activated kinase (AMPK), another element downstream of cAMP signaling whose activation inhibits HSL activity, was also not increased by AIM or C75 (Figure S8C).

DISCUSSION

A Role of AIM in Adipocytes

Our present results provide several findings regarding the influence of AIM on adipocytes. First, AIM is endocytosed into adipocytes via CD36. Second, incorporated AIM binds to cytosolic FAS protein at various regions responsible for elongation of fatty acids, release of synthesized palmitate, and stabilization of FAS dimerization. This results in a decrease in FAS enzymatic activity. Third, the decrease in FAS activity induced by AIM results in a decrease in lipid droplet storage within adipocytes. Finally, the size of adipocytes in visceral fat tissue is increased in $AIM^{-/-}$ mice compared to $AIM^{+/+}$ mice. The physiologic consequence of the lipolytic response induced by AIM remains to be investigated. It is possible that AIM resists augmentation of adipose tissue mass, leading to decreased progression of obesity. Indeed, the increase in weight of visceral fat in mice fed with a HFD was accelerated in $AIM^{-/-}$ mice compared to $AIM^{+/+}$ mice (Figure 5B), and it was suppressed by the systemic administration of rAIM (Figure 5C). Importantly, this antiadiposity function of AIM appears to be exerted specifically via its effect on adipocytes, because both $AIM^{-/-}$ and $AIM^{+/+}$ mice showed comparable metabolic rates (Figure S5). Additional discussion related to this issue appears in the Supplemental Information online.

Direct Function of AIM in the Absence of Signaling

Interestingly, exogenous AIM secreted by macrophages is incorporated into adipocytes and directly functions intracellularly. Such a direct manner of function in the absence of signaling is unusual in a secreted molecule. However, examples in which cytosolic delivery of exogenous proteins mediates biological effects have recently been accumulating. Fibroblast growth factor (FGF)-1 and -2 (Olsnes et al., 2003; Wesche et al., 2006) as well as epidermal growth factor (EGF) (Lin et al., 2001) are transported to the cytosol after internalization via specific receptors, where they trigger cellular events. In addition, many plant and bacterial toxins, such as ricin and Shiga toxin, are also endocytosed by eukaryotic cells in a receptor-dependent manner and are translocated into the cytosol to target-specific intracellular proteins (Sandvig and van Deurs, 2000, 2005). It is also known that in dendritic cells, some exogenous antigens can access the cytosol via similar machineries for intracellular transport and are presented by major histocompatibility complex (MHC) class I (Ackerman et al., 2005; Giodini and Cresswell, 2008). Yet it remains unclear how AIM is translocated from endosomal compartments to the cytosol. Interestingly, incorporated AIM colocalized with early endosomes but not with late or recycling endosomes (Figure 3B). This observation implicates the presence of a specific mechanism to transport AIM from endosomes

Figure 3. AIM Is Endocytosed via CD36

(A) Differentiated 3T3-L1 adipocytes (ins/DEX/IBMX stimulation +) or undifferentiated 3T3-L1 preadipocytes without maturation stimulation (ins/DEX/IBMX stimulation −) were incubated with rAIM (5 μg/ml) for 3 hr and stained for AIM (red), PPARγ2 (green), and DAPI (blue). Top panels, AIM + DAPI; middle panels, AIM + PPARγ2; bottom panels, AIM + PPARγ2 + DAPI (merged), overlaid with phase-contrast images. In the bottom panels, cells showing strong PPARγ2 positivity contained many lipid droplets. Yellow arrows, mature 3T3-L1 adipocytes showing strong staining for PPARγ2; blue arrows, cells showing faint staining for PPARγ2; white arrows, cells showing undetectable staining for PPARγ2. Right lane (pre): undifferentiated 3T3-L1 preadipocytes without stimulation. The percentage of cells showing AIM incorporation was calculated for 100 cells of each type (graph under photomicrographs; rAIM incorporation). Results were obtained from three independent experiments.

(B) 3T3-L1 adipocytes treated with rAIM for 3 hr were costained for AIM (red) and early, late, or recycling endosomes (green: with antibody to EEA1, Rab7, or Rab11, respectively); AIM (green) and lysosomes (red: LysoTracker Red DND-99); and AIM (green) and lipid droplets (red: Nile Red). Specimens were observed under a confocal microscope.

(C) Electron microscopic analysis of the same cell samples after immunogold labeling of AIM. E, endosome; N, nucleus. Scales are indicated by bars.

(D) Treatment of 3T3-L1 adipocytes with CD36-neutralizing antibody inhibited endocytosis of rAIM. Incorporation of rAIM was assessed in cells treated with α-CD36 antibody or control mouse IgA. A total of 100 cells were evaluated for each treatment. Results were obtained from three independent experiments.

(E) Defective uptake of AIM by $CD36^{-/-}$ adipocytes. rAIM (300 μg/mouse in phosphate-buffered saline) was i.v. injected into $CD36^{+/+}$ and $CD36^{-/-}$ mice. At 16 hr after injection, mice were sacrificed and sections were prepared from epididymal fat tissue. Sections were stained for AIM (green: upper panels) and macrophages F4/80 (red: middle panels).

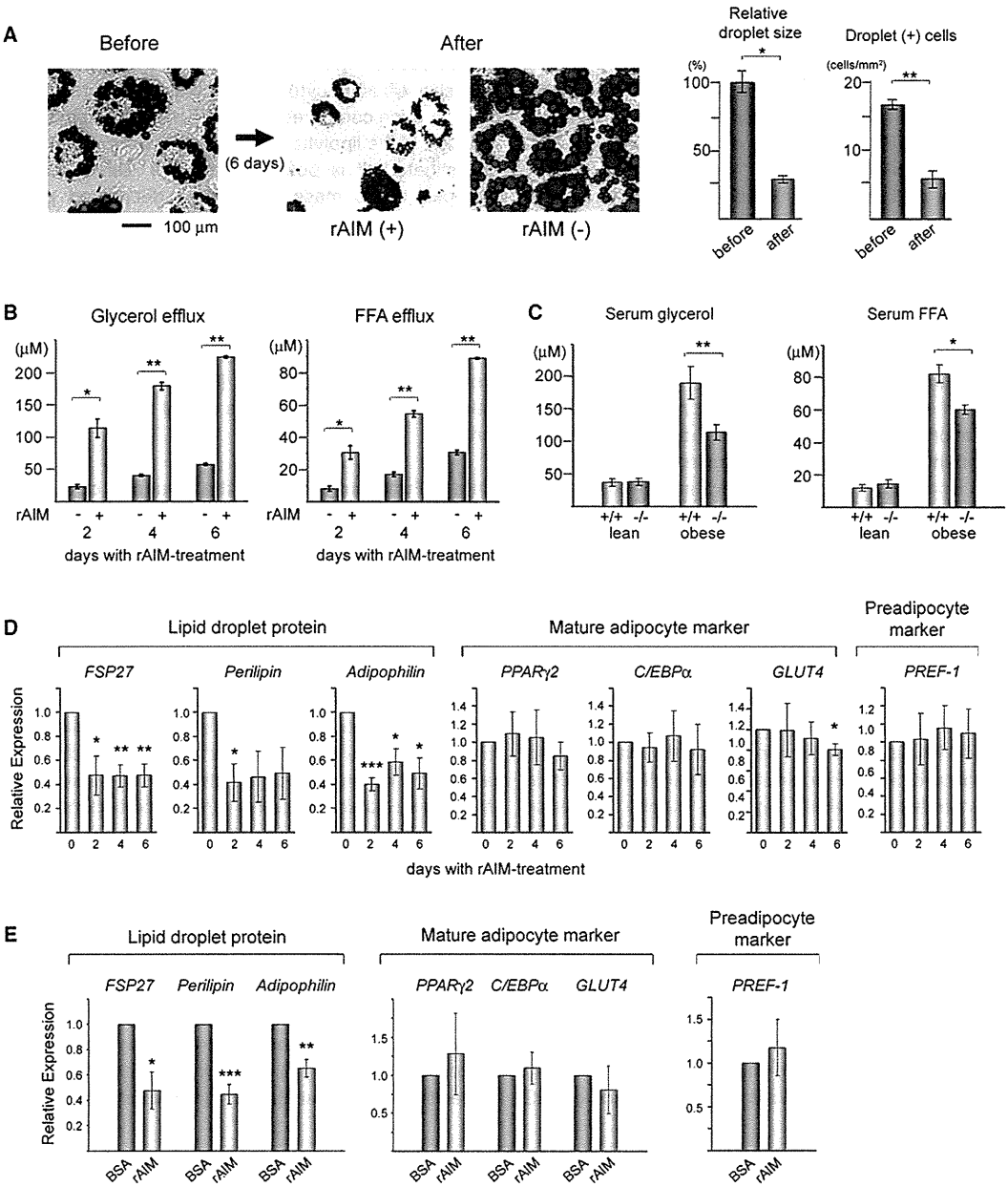

Figure 4. AIM Induces a Lipolytic Response

(A) Differentiated 3T3-L1 adipocytes were challenged with rAIM (5 μg/ml) for 6 days. Cells were stained with Oil Red O before and after rAIM treatment. Representative photomicrographs of cells before and after treatment with or without rAIM (5 μg/ml) are presented. Relative droplet size was assessed by evaluating the diameter of 50 droplets. Error bar indicates SEM. The numbers of droplet-containing cells are also shown (cells/mm^2). Data are presented as the means of five independent areas. Error bar indicates SEM. Before, before rAIM treatment; After, after 6 day rAIM treatment.

(B) Efflux of glycerol and FFAs after culture of 3T3-L1 adipocytes with or without rAIM (5 μg/ml) for 2, 4, or 6 days. Data are shown as culture supernatant concentrations. Three independent experiments were performed. Error bar indicates SEM.

(C) Basal levels of glycerol and FFAs in serum from lean (fed with normal chow) and obese (fed with a HFD for 20 weeks) *AIM*$^{+/+}$ and *AIM*$^{-/-}$ mice. n = 6 for each group. Error bar indicates SEM.

(D) 3T3-L1 adipocytes incubated with rAIM (5 μg/ml) for 0, 2, 4, or 6 days were analyzed for mRNA levels of *FSP27*, *Perilipin*, *Adipophilin*, *PPARγ2*, *C/EBPα*, *GLUT4*, and *PREF-1* by quantitative PCR. Values were normalized to those of *glyceraldehyde 3-phosphate dehydrogenase* (*GAPDH*) and presented as relative expression to that for the 0 day rAIM treatment. Three independent experiments were performed. Error bar indicates SEM.

(E) In vivo experiment. The mRNA levels of the same genes as in (D) were assessed by QPCR with RNA isolated from epididymal fat in *AIM*$^{-/-}$ mice after direct injection of rAIM (100 μg/whole tissue) or BSA (same amount) into the fat tissues (n = 7 for each). Values were normalized to those of *GAPDH* and presented as relative expression to that from fat tissues injected with BSA. Error bar indicates SEM.

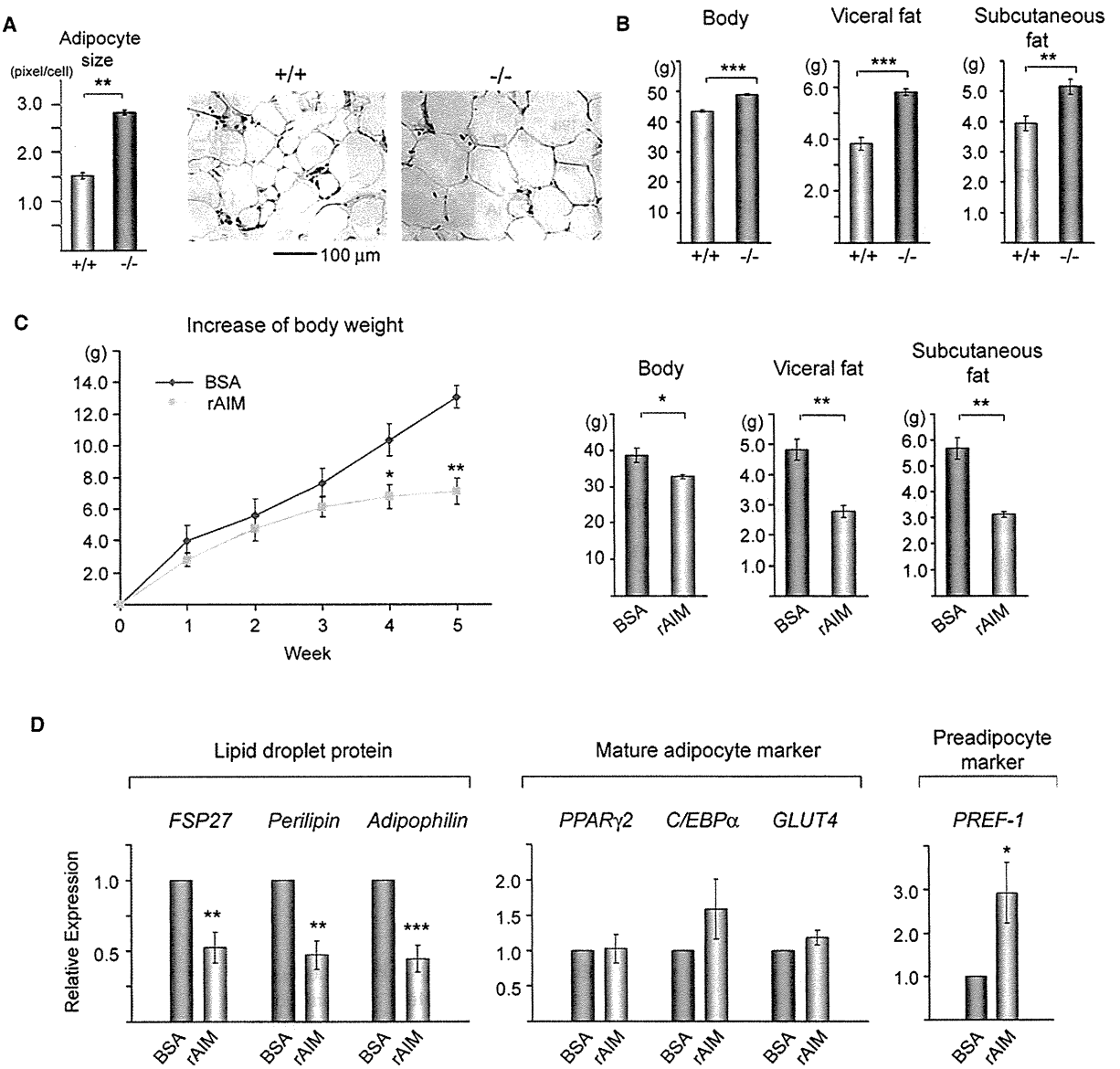

Figure 5. AIM Influences Adipose Tissue Mass

(A) Adipocyte size. In $AIM^{+/+}$ mice (+/+) and $AIM^{-/-}$ mice (−/−) (both fed with a HFD for 20 weeks), epididymal fat sections were stained with H&E, and the diameter of 50 independent adipocytes in different areas was evaluated. Results are presented as averages ± SEM (in pixels). Representative photomicrographs of adipose tissues are also presented.

(B) Weights for body, visceral fat tissue, and subcutaneous fat tissue from $AIM^{+/+}$ mice (+/+) and $AIM^{-/-}$ mice (−/−) fed with a HFD for 12 weeks. n = 7 for $AIM^{+/+}$, and n = 6 for $AIM^{-/-}$. Error bar indicates SEM.

(C) $AIM^{-/-}$ mice were fed with a HFD for 5 weeks, and during the period, they were i.p. injected with rAIM or BSA twice a week (300 μg/injection/mouse). The increase in body weight at each week (line graph) and overall body weight and weight of visceral and subcutaneous fat tissues at the end of experiment (bar graphs) are presented. n = 6 for rAIM-injected mice, and n = 5 for BSA-injected mice. Error bar indicates SEM.

(D) mRNA levels of *FSP27*, *Perilipin* and *Adipophilin*, *PPARγ2*, *C/EBPα*, *GLUT4*, and *PREF-1* were assessed by QPCR with RNA isolated from epididymal fat from mice used in (C) at the end of the experiment. Values were normalized to those of *GAPDH* and presented as relative expression to that of fat tissue injected with BSA. n = 6 for rAIM-injected mice and n = 5 for BSA-injected mice. Error bar indicates SEM.

to the cytoplasm. It is possible that a certain cytosolic chaperone is required, as it has recently been found that the efficient translocation of some proteins across the endosomal membrane is dependent on Hsp90 (Haug et al., 2003; Ratts et al., 2003; Wesche et al., 2006; Giodini and Cresswell, 2008). Additional experiments are necessary to clarify the mechanism responsible for AIM translocation from the endosomal compartment to the cytosol.

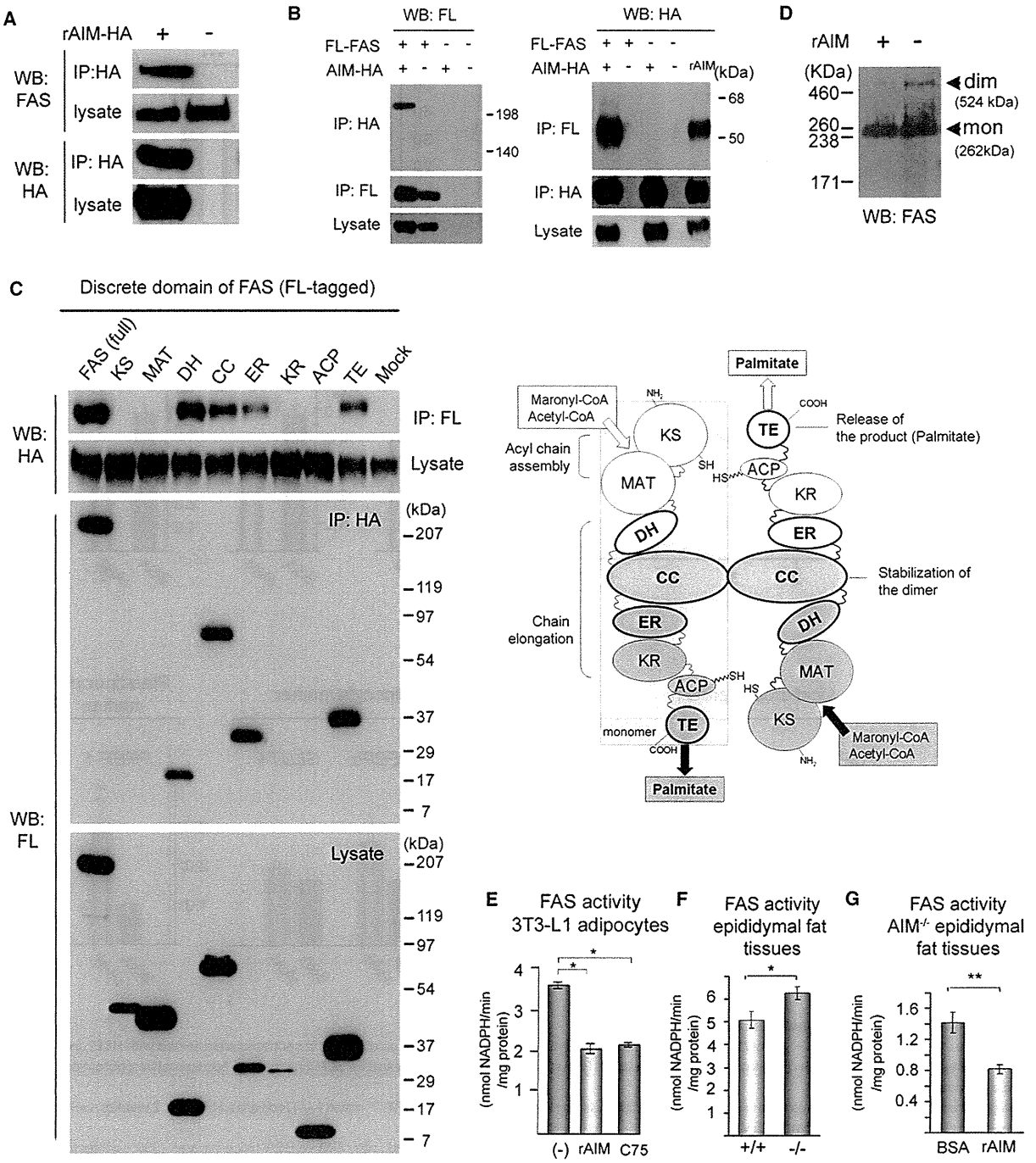

Figure 6. AIM Targets FAS

(A) *AIM*$^{-/-}$ mice were injected with rAIM (HA tagged) directly into the epididymal fat (total 100 μg at several loci). Three hours after injection, fat tissues were used to test the association of incorporated rAIM-HA and endogenous cytosolic FAS in fat tissues via coIP using anti-HA antibody. Precipitates were analyzed for the presence of FAS by western blotting (WB).

(B) Association of rAIM (HA tagged) and FAS (FLAG tagged) in HEK293T cells as determined by coIP assay using anti-Flag or anti-HA antibody.

(C) Left: Each domain of FAS was tagged with the Flag sequence at the N terminus and expressed in HEK293T cells stably expressing AIM-HA, and their association was determined by a coIP assay using anti-Flag or anti-HA antibody. Overexpression of ER or KR domains of FAS resulted in death of a large number of cells. This caused a decrease in WB signals using these cell lysates (lower panels, lanes ER and KR). Results from IP-FL/WB-FL, IP-HA/WB-HA, and IP-control IgG (rat or mouse)/WB-FL or -HA are presented in Figure S6. Right: A schematic of head-to-tail dimerized FAS and descriptions of the major function for each region. Two functional units (distinguished by white and gray) are located on the axis of bound CCs. The AIM-binding domains (DH, CC, ER, and TE) are indicated

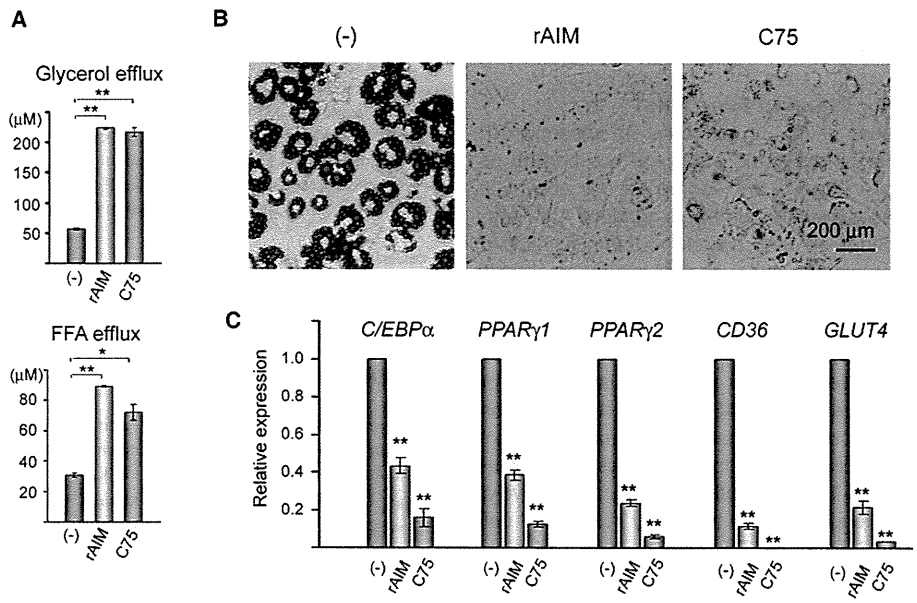

Figure 7. AIM and C75 Exert Comparable Effects on Adipocytes

(A) rAIM (5 μg/ml) or C75 (25 μM) was added to differentiated 3T3-L1 adipocytes for 6 days, and the efflux of glycerol and FFAs was evaluated. Three independent experiments were performed. Error bar indicates SEM.

(B) Both AIM and C75 inhibited adipogenesis. 3T3-L1 preadipocytes were challenged with rAIM (5 μg/ml) or C75 (25 μM) for 2 days during stimulation of differentiation by insulin, DEX, and IBMX. At day 12 of culture, cells were stained with Oil Red O. In the presence of rAIM or C75, adipocyte differentiation was completely prevented.

(C) Gene expression profiles at day 12 of culture. Total RNA was isolated from cells, and the mRNA levels for the indicated genes were assessed by QPCR (n = 3 for each group). Values were normalized to those of *GAPDH* and presented as relative expression to that of cells cultured in the absence of rAIM or C75. Error bar indicates SEM.

FAS as a Target Molecule of Incorporated AIM in Adipocytes

It is of interest that a functional target of AIM is FAS. Through association with multiple regions of FAS (Figure 6C), AIM appears to decrease FAS activity functionally and structurally. The effect of FAS inhibition on the hypothalamus, which influences the fat mass in the body, has been studied extensively. Evidence indicates that systemic administration of C75 decreases the production of neuropeptide Y (NP-Y) in the hypothalamus in mice, resulting in a marked loss of appetite and overall decreased body weight (Loftus et al., 2000; Makimura et al., 2001; Kumar et al., 2002; Mobbs and Makimura, 2002; Shimokawa et al., 2002; Kovacs et al., 2004; Liu et al., 2004; Ronnett et al., 2005; Chakravarthy et al., 2009a). However, $AIM^{-/-}$ and $AIM^{+/+}$ mice showed comparable levels of food intake (Figure S5), suggesting that AIM may not have a neurologic effect. This may be due to the requirement of a specific endocytotic process mediated by CD36, the expression of which is not reported in hypothalamic cells.

Instead, our present results indicate a direct effect of FAS inhibition on adipocytes (brought about by either AIM or C75), which decreases the size and number of lipid droplets, thereby decreasing adipocyte size. There are several possibilities for the mechanism of FAS inhibition in the lipolytic response. Because the inhibition of FAS did not stimulate the cAMP/PKA signaling cascade (Figure S8), it might activate an unknown cAMP/PKA-independent lipolytic pathway. Alternatively, because differentiating adipocytes or mice on a HFD undergo progressive lipogenesis (increase in lipid droplet storage) and constitutive (basal) lipolysis at a substantial level (Holm, 2003; Zechner et al., 2005; Duncan et al., 2007; Lafontan, 2008), the lipolytic outcome on FAS inhibition might simply represent an acute disturbance of lipogenesis. Indeed, it is well known that de novo synthesis of fatty acids via FAS is indispensable for efficient lipogenesis

in bold. A monomer FAS molecule is indicated by a shadowed square. KS, ketoacyl synthase; MAT, malonyl/acetyl transferase; DH, dehydrase; CC, central core; ER, enoylreductase; KR, ketoreductase; ACP, acyl carrier protein; TE, thioesterase.

(D) Dimerized FAS is decreased in the presence of AIM. Cell lysates from 3T3-L1 adipocytes maintained with or without rAIM (5 μg/ml) for 2 days were run on a Tris-acetate gel, and immunoblotting was carried out to assess dimerized (524 kDa) and monomeric (262 kDa) FAS. Sodium dodecyl sulfate (SDS) was removed from the loading buffer to limit potential degradation of the dimerized form.

(E–G) FAS activity in 3T3-L1 adipocytes treated with or without rAIM (5 μg/ml) or C75 (25 μM) for 6 days (E), epididymal fat tissues from $AIM^{+/+}$ and $AIM^{-/-}$ mice (F), and $AIM^{-/-}$ epididymal fat tissue challenged with a local intrafat injection of rAIM or BSA (total 100 μg for each at several loci within the tissue) 3 hr before analysis (G). All mice were fed with a HFD for 20 weeks. Samples were lysed and analyzed for FAS activity. Data are presented for normalized FAS protein levels as assessed by WB using the same samples (data not shown). n = 6 for each group. Error bar indicates SEM.

(Lafontan, 2008). Further discussion related to this issue appears in the Supplemental Information online.

Same Mechanism for Different Functions?

Whether other functions of AIM, in particular its antiapoptotic effect, are carried out by the same molecular mechanism as that in adipocytes will need to be addressed. As shown in Figure 2B, macrophages also incorporate exogenous AIM, suggesting that AIM functions in macrophages in a manner similar to that in adipocytes. Intriguingly, although AIM inhibits apoptosis in macrophages (Miyazaki et al., 1999; Arai et al., 2005), evidence has shown that suppression of FAS promoted apoptosis in some cancer cells (Lupu and Menendez, 2006; Menendez and Lupu, 2007). However, whether apoptosis is inhibited or accelerated by the suppression of FAS might be dependent on cell type. Certainly, in some cell types, the overexpression of FAS accelerated apoptosis, upregulating the expression of proapoptotic genes (J.K. and T.M., unpublished data). Alternatively, intracellular target molecules of AIM may vary in different cell types and/or in different situations. The mediators for AIM internalization might also vary, given that thymocytes and NK-T cells, in which AIM is also effective (Miyazaki et al., 1999; Kuwata et al., 2003), do not express CD36. This may explain the multiple functions observed for AIM in many cell types.

Perspectives

In conclusion, we have identified a function of AIM, along with its molecular mechanism, with respect to adipocyte status in fat tissue. The effects of AIM on other organs important for metabolism, such as liver and muscle, remain to be determined. Further investigation will provide new insights into the role of AIM in the pathogenesis of obesity as well as metabolic diseases.

EXPERIMENTAL PROCEDURES

Mice

AIM$^{-/-}$ mice (Miyazaki et al., 1999) had been backcrossed to C57BL/6 (B6) for 13 generations before being used for experiments. *CD36*$^{-/-}$ mice (Febbraio et al., 1999) were created and maintained by Febbraio in the Lerner Research Institute, Cleveland Clinic Foundation. All mice were maintained under a specific pathogen-free (SPF) condition.

Statistical Analysis

A two-tailed Mann-Whitney test was used to calculate p values. ***$p < 0.001$, **$p < 0.01$, *$p < 0.05$. Error bars indicate SEM.

Detailed description about reagents for histological analysis, purification of rAIM, in vitro adipogenesis, FAS constructs, efflux analysis of glycerol and FFAs, silver-intensified immunogold for electron microscopy, FAS activity assay, analysis of metabolic rates, quantitative PCR assay, and primers used for experiments appears in the Supplemental Information online.

SUPPLEMENTAL INFORMATION

Supplemental Information includes Supplemental Discussion, Supplemental Experimental Procedures, Supplemental References, and eight figures and can be found with this article online at doi:10.1016/j.cmet.2010.04.013.

ACKNOWLEDGMENTS

We thank O. Ohara (Chiba), T. Fujita (Niigata), and T. Ide (Saitama) for useful advice; K. Ikeda and R. Taguchi (Tokyo) as well as Genostaff, Inc. for technical assistance in histology; and M. Egami and M. Miyamoto for preparing the manuscript. This work was supported by Grants-in-Aid for Scientific Research, the Global COE Research Program, Takeda Science Foundation, Research Fund of Mitsukoshi Health and Welfare Foundation, Sankyo Foundation of Life Science, Mitsubishi Pharma Research Foundation, The Mochida Memorial Foundation for Medical and Pharmaceutical Research, Uehara Memorial Foundation, Suzuken Memorial Foundation (to T.M.), Kanae Foundation for the Promotion of Medical Science, Astellas Foundation for Research on Metabolic Disorders, and Ono Medical Research Foundation (to S.A.).

Received: September 14, 2009
Revised: December 18, 2009
Accepted: April 19, 2010
Published: June 8, 2010

REFERENCES

Ackerman, A.L., Kyritsis, C., Tampé, R., and Cresswell, P. (2005). Access of soluble antigens to the endoplasmic reticulum can explain cross-presentation by dendritic cells. Nat. Immunol. *6*, 107–113.

Apovian, C.M., Bigornia, S., Mott, M., Meyers, M.R., Ulloor, J., Gagua, M., McDonnell, M., Hess, D., Joseph, L., and Gokce, N. (2008). Adipose macrophage infiltration is associated with insulin resistance and vascular endothelial dysfunction in obese subjects. Arterioscler. Thromb. Vasc. Biol. *28*, 1654–1659.

Arai, S., Shelton, J.M., Chen, M., Bradley, M.N., Castrillo, A., Bookout, A.L., Mak, P.A., Edwards, P.A., Mangelsdorf, D.J., Tontonoz, P., and Miyazaki, T. (2005). A role for the apoptosis inhibitory factor AIM/Spalpha/Api6 in atherosclerosis development. Cell Metab. *1*, 201–213.

Asturias, F.J., Chadick, J.Z., Cheung, I.K., Stark, H., Witkowski, A., Joshi, A.K., and Smith, S. (2005). Structure and molecular organization of mammalian fatty acid synthase. Nat. Struct. Mol. Biol. *12*, 225–232.

Baker, J.L., Olsen, L.W., and Sørensen, T.I. (2007). Childhood body-mass index and the risk of coronary heart disease in adulthood. N. Engl. J. Med. *357*, 2329–2337.

Brake, D.K., Smith, E.O., Mersmann, H., Smith, C.W., and Robker, R.L. (2006). ICAM-1 expression in adipose tissue: effects of diet-induced obesity in mice. Am. J. Physiol. Cell Physiol. *291*, C1232–C1239.

Chakravarthy, M.V., Zhu, Y., Yin, L., Coleman, T., Pappan, K.L., Marshall, C.A., McDaniel, M.L., and Semenkovich, C.F. (2009a). Inactivation of hypothalamic FAS protects mice from diet-induced obesity and inflammation. J. Lipid Res. *50*, 630–640.

Chirala, S.S., Chang, H., Matzuk, M., Abu-Elheiga, L., Mao, J., Mahon, K., Finegold, M., and Wakil, S.J. (2003). Fatty acid synthesis is essential in embryonic development: fatty acid synthase null mutants and most of the heterozygotes die in utero. Proc. Natl. Acad. Sci. USA *100*, 6358–6363.

Cinti, S., Mitchell, G., Barbatelli, G., Murano, I., Ceresi, E., Faloia, E., Wang, S., Fortier, M., Greenberg, A.S., and Obin, M.S. (2005). Adipocyte death defines macrophage localization and function in adipose tissue of obese mice and humans. J. Lipid Res. *46*, 2347–2355.

Ducharme, N.A., and Bickel, P.E. (2008). Lipid droplets in lipogenesis and lipolysis. Endocrinology *149*, 942–949.

Duncan, R.E., Ahmadian, M., Jaworski, K., Sarkadi-Nagy, E., and Sul, H.S. (2007). Regulation of lipolysis in adipocytes. Annu. Rev. Nutr. *27*, 79–101.

Farmer, S.R. (2006). Transcriptional control of adipocyte formation. Cell Metab. *4*, 263–273.

Febbraio, M., Abumrad, N.A., Hajjar, D.P., Sharma, K., Cheng, W., Pearce, S.F., and Silverstein, R.L. (1999). A null mutation in murine CD36 reveals an important role in fatty acid and lipoprotein metabolism. J. Biol. Chem. *274*, 19055–19062.

Finn, P.F., and Dice, J.F. (2006). Proteolytic and lipolytic responses to starvation. Nutrition *22*, 830–844.

Gangadharan, B., Antrobus, R., Dwek, R.A., and Zitzmann, N. (2007). Novel serum biomarker candidates for liver fibrosis in hepatitis C patients. Clin. Chem. *53*, 1792–1799.

Gebe, J.A., Kiener, P.A., Ring, H.Z., Li, X., Francke, U., and Aruffo, A. (1997). Molecular cloning, mapping to human chromosome 1 q21-q23, and cell binding characteristics of Spalpha, a new member of the scavenger receptor cysteine-rich (SRCR) family of proteins. J. Biol. Chem. *272*, 6151–6158.

Gebe, J.A., Llewellyn, M., Hoggatt, H., and Aruffo, A. (2000). Molecular cloning, genomic organization and cell-binding characteristics of mouse Spalpha. Immunology *99*, 78–86.

Giodini, A., and Cresswell, P. (2008). Hsp90-mediated cytosolic refolding of exogenous proteins internalized by dendritic cells. EMBO J. *27*, 201–211.

Gray, J., Chattopadhyay, D., Beale, G.S., Patman, G.L., Miele, L., King, B.P., Stewart, S., Hudson, M., Day, C.P., Manas, D.M., and Reeves, H.L. (2009). A proteomic strategy to identify novel serum biomarkers for liver cirrhosis and hepatocellular cancer in individuals with fatty liver disease. BMC Cancer *9*, 271.

Greenwalt, D.E., Lipsky, R.H., Ockenhouse, C.F., Ikeda, H., Tandon, N.N., and Jamieson, G.A. (1992). Membrane glycoprotein CD36: a review of its roles in adherence, signal transduction, and transfusion medicine. Blood *80*, 1105–1115.

Haug, G., Leemhuis, J., Tiemann, D., Meyer, D.K., Aktories, K., and Barth, H. (2003). The host cell chaperone Hsp90 is essential for translocation of the binary Clostridium botulinum C2 toxin into the cytosol. J. Biol. Chem. *278*, 32266–32274.

He, W., Barak, Y., Hevener, A., Olson, P., Liao, D., Le, J., Nelson, M., Ong, E., Olefsky, J.M., and Evans, R.M. (2003). Adipose-specific peroxisome proliferator-activated receptor gamma knockout causes insulin resistance in fat and liver but not in muscle. Proc. Natl. Acad. Sci. USA *100*, 15712–15717.

Holm, C. (2003). Molecular mechanisms regulating hormone-sensitive lipase and lipolysis. Biochem. Soc. Trans. *31*, 1120–1124.

Ibrahimi, A., and Abumrad, N.A. (2002). Role of CD36 in membrane transport of long-chain fatty acids. Curr. Opin. Clin. Nutr. Metab. Care *5*, 139–145.

Joseph, S.B., Bradley, M.N., Castrillo, A., Bruhn, K.W., Mak, P.A., Pei, L., Hogenesch, J., O'connell, R.M., Cheng, G., Saez, E., et al. (2004). LXR-dependent gene expression is important for macrophage survival and the innate immune response. Cell *119*, 299–309.

Kelley, D.S., Nelson, G.J., and Hunt, J.E. (1986). Effect of prior nutritional status on the activity of lipogenic enzymes in primary monolayer cultures of rat hepatocytes. Biochem. J. *235*, 87–90.

Kim, W.K., Hwang, H.R., Kim, H., Lee, P.Y., In, Y.J., Ryu, H.Y., Park, S.G., Bae, K.H., and Lee, S.C. (2008). Glycoproteomic analysis of plasma from patients with atopic dermatitis: CD5L and ApoE as potential biomarkers. Exp. Mol. Med. *40*, 677–685.

Kovacs, P., Harper, I., Hanson, R.L., Infante, A.M., Bogardus, C., Tataranni, P.A., and Baier, L.J. (2004). A novel missense substitution (Val1483Ile) in the fatty acid synthase gene (FAS) is associated with percentage of body fat and substrate oxidation rates in nondiabetic Pima Indians. Diabetes *53*, 1915–1919.

Kuhajda, F.P., Pizer, E.S., Li, J.N., Mani, N.S., Frehywot, G.L., and Townsend, C.A. (2000). Synthesis and antitumor activity of an inhibitor of fatty acid synthase. Proc. Natl. Acad. Sci. USA *97*, 3450–3454.

Kumar, M.V., Shimokawa, T., Nagy, T.R., and Lane, M.D. (2002). Differential effects of a centrally acting fatty acid synthase inhibitor in lean and obese mice. Proc. Natl. Acad. Sci. USA *99*, 1921–1925.

Kuwata, K., Watanabe, H., Jiang, S.Y., Yamamoto, T., Tomiyama-Miyaji, C., Abo, T., Miyazaki, T., and Naito, M. (2003). AIM inhibits apoptosis of T cells and NKT cells in Corynebacterium-induced granuloma formation in mice. Am. J. Pathol. *162*, 837–847.

Lafontan, M. (2008). Advances in adipose tissue metabolism. Int. J Obes. (Lond) *32* (*Suppl 7*), S39–S51.

Lin, S.Y., Makino, K., Xia, W., Matin, A., Wen, Y., Kwong, K.Y., Bourguignon, L., and Hung, M.C. (2001). Nuclear localization of EGF receptor and its potential new role as a transcription factor. Nat. Cell Biol. *3*, 802–808.

Liu, L.H., Wang, X.K., Hu, Y.D., Kang, J.L., Wang, L.L., and Li, S. (2004). Effects of a fatty acid synthase inhibitor on adipocyte differentiation of mouse 3T3-L1 cells. Acta Pharmacol. Sin. *25*, 1052–1057.

Loftus, T.M., Jaworsky, D.E., Frehywot, G.L., Townsend, C.A., Ronnett, G.V., Lane, M.D., and Kuhajda, F.P. (2000). Reduced food intake and body weight in mice treated with fatty acid synthase inhibitors. Science *288*, 2379–2381.

Lupu, R., and Menendez, J.A. (2006). Pharmacological inhibitors of Fatty Acid Synthase (FASN)—catalyzed endogenous fatty acid biogenesis: a new family of anti-cancer agents? Curr. Pharm. Biotechnol. *7*, 483–493.

Madsen, L., Petersen, R.K., Sørensen, M.B., Jørgensen, C., Hallenborg, P., Pridal, L., Fleckner, J., Amri, E.Z., Krieg, P., Furstenberger, G., et al. (2003). Adipocyte differentiation of 3T3-L1 preadipocytes is dependent on lipoxygenase activity during the initial stages of the differentiation process. Biochem. J. *375*, 539–549.

Makimura, H., Mizuno, T.M., Yang, X.J., Silverstein, J., Beasley, J., and Mobbs, C.V. (2001). Cerulenin mimics effects of leptin on metabolic rate, food intake, and body weight independent of the melanocortin system, but unlike leptin, cerulenin fails to block neuroendocrine effects of fasting. Diabetes *50*, 733–739.

Menendez, J.A., and Lupu, R. (2007). Fatty acid synthase and the lipogenic phenotype in cancer pathogenesis. Nat. Rev. Cancer *7*, 763–777.

Miyazaki, T., Hirokami, Y., Matsuhashi, N., Takatsuka, H., and Naito, M. (1999). Increased susceptibility of thymocytes to apoptosis in mice lacking AIM, a novel murine macrophage-derived soluble factor belonging to the scavenger receptor cysteine-rich domain superfamily. J. Exp. Med. *189*, 413–422.

Mobbs, C.V., and Makimura, H. (2002). Block the FAS, lose the fat. Nat. Med. *8*, 335–336.

Neels, J.G., and Olefsky, J.M. (2006). Inflamed fat: what starts the fire? J. Clin. Invest. *116*, 33–35.

Nishino, N., Tamori, Y., Tateya, S., Kawaguchi, T., Shibakusa, T., Mizunoya, W., Inoue, K., Kitazawa, R., Kitazawa, S., Matsuki, Y., et al. (2008). FSP27 contributes to efficient energy storage in murine white adipocytes by promoting the formation of unilocular lipid droplets. J. Clin. Invest. *118*, 2808–2821.

Olshansky, S.J., Passaro, D.J., Hershow, R.C., Layden, J., Carnes, B.A., Brody, J., Hayflick, L., Butler, R.N., Allison, D.B., and Ludwig, D.S. (2005). A potential decline in life expectancy in the United States in the 21st century. N. Engl. J. Med. *352*, 1138–1145.

Olsnes, S., Klingenberg, O., and Wiedłocha, A. (2003). Transport of exogenous growth factors and cytokines to the cytosol and to the nucleus. Physiol. Rev. *83*, 163–182.

Puri, V., and Czech, M.P. (2008). Lipid droplets: FSP27 knockout enhances their sizzle. J. Clin. Invest. *118*, 2693–2696.

Qu, P., Du, H., Li, Y., and Yan, C. (2009). Myeloid-specific expression of Api6/AIM/Sp alpha induces systemic inflammation and adenocarcinoma in the lung. J. Immunol. *182*, 1648–1659.

Ratts, R., Zeng, H., Berg, E.A., Blue, C., McComb, M.E., Costello, C.E., vanderSpek, J.C., and Murphy, J.R. (2003). The cytosolic entry of diphtheria toxin catalytic domain requires a host cell cytosolic translocation factor complex. J. Cell Biol. *160*, 1139–1150.

Ronnett, G.V., Kim, E.K., Landree, L.E., and Tu, Y. (2005). Fatty acid metabolism as a target for obesity treatment. Physiol. Behav. *85*, 25–35.

Rosen, E.D., Sarraf, P., Troy, A.E., Bradwin, G., Moore, K., Milstone, D.S., Spiegelman, B.M., and Mortensen, R.M. (1999). PPAR gamma is required for the differentiation of adipose tissue in vivo and in vitro. Mol. Cell *4*, 611–617.

Sandvig, K., and van Deurs, B. (2000). Entry of ricin and Shiga toxin into cells: molecular mechanisms and medical perspectives. EMBO J. *19*, 5943–5950.

Sandvig, K., and van Deurs, B. (2005). Delivery into cells: lessons learned from plant and bacterial toxins. Gene Ther. *12*, 865–872.

Schmid, B., Rippmann, J.F., Tadayyon, M., and Hamilton, B.S. (2005). Inhibition of fatty acid synthase prevents preadipocyte differentiation. Biochem. Biophys. Res. Commun. *328*, 1073–1082.

Shimokawa, T., Kumar, M.V., and Lane, M.D. (2002). Effect of a fatty acid synthase inhibitor on food intake and expression of hypothalamic neuropeptides. Proc. Natl. Acad. Sci. USA *99*, 66–71.

Shoelson, S.E., Lee, J., and Goldfine, A.B. (2006). Inflammation and insulin resistance. J. Clin. Invest. *116*, 1793–1801.

Smas, C.M., and Sul, H.S. (1993). Pref-1, a protein containing EGF-like repeats, inhibits adipocyte differentiation. Cell *73*, 725–734.

Smith, S. (1994). The animal fatty acid synthase: one gene, one polypeptide, seven enzymes. FASEB J. *8*, 1248–1259.

Smith, S., Stern, A., Randhawa, Z.I., and Knudsen, J. (1985). Mammalian fatty acid synthetase is a structurally and functionally symmetrical dimer. Eur. J. Biochem. *152*, 547–555.

Surmi, B.K., and Hasty, A.H. (2008). Macrophage infiltration into adipose tissue: initiation, propagation and remodeling. Future Lipidol. *3*, 545–556.

Valledor, A.F., Hsu, L.C., Ogawa, S., Sawka-Verhelle, D., Karin, M., and Glass, C.K. (2004). Activation of liver X receptors and retinoid X receptors prevents bacterial-induced macrophage apoptosis. Proc. Natl. Acad. Sci. USA *101*, 17813–17818.

Wesche, J., Małecki, J., Wiedłocha, A., Skjerpen, C.S., Claus, P., and Olsnes, S. (2006). FGF-1 and FGF-2 require the cytosolic chaperone Hsp90 for translocation into the cytosol and the cell nucleus. J. Biol. Chem. *281*, 11405–11412.

Wu, Z., Puigserver, P., and Spiegelman, B.M. (1999a). Transcriptional activation of adipogenesis. Curr. Opin. Cell Biol. *11*, 689–694.

Wu, Z., Rosen, E.D., Brun, R., Hauser, S., Adelmant, G., Troy, A.E., McKeon, C., Darlington, G.J., and Spiegelman, B.M. (1999b). Cross-regulation of C/EBP alpha and PPAR gamma controls the transcriptional pathway of adipogenesis and insulin sensitivity. Mol. Cell *3*, 151–158.

Yusa, S., Ohnishi, S., Onodera, T., and Miyazaki, T. (1999). AIM, a murine apoptosis inhibitory factor, induces strong and sustained growth inhibition of B lymphocytes in combination with TGF-β1. Eur. J. Immunol. *29*, 1086–1093.

Zechner, R., Strauss, J.G., Haemmerle, G., Lass, A., and Zimmermann, R. (2005). Lipolysis: pathway under construction. Curr. Opin. Lipidol. *16*, 333–340.

Biochemical and Biophysical Research Communications 391 (2010) 1708–1713

Contents lists available at ScienceDirect

Biochemical and Biophysical Research Communications

journal homepage: www.elsevier.com/locate/ybbrc

The death effector domain-containing DEDD forms a complex with Akt and Hsp90, and supports their stability

Nobuya Kurabe [1], Mayumi Mori, Jun Kurokawa, Kaori Taniguchi, Hisatoshi Aoyama, Kazuhiro Atsuda, Akemi Nishijima, Nariaki Odawara, Saori Harada, Katsuhiko Nakashima, Satoko Arai, Toru Miyazaki *

Division of Molecular Biomedicine for Pathogenesis, Center for Disease Biology and Integrative Medicine, Faculty of Medicine, The University of Tokyo, 7-3-1, Hongo, Bunkyo-ku, Tokyo 113-0033, Japan

ARTICLE INFO

Article history:
Received 22 December 2009
Available online 30 December 2009

Keywords:
DEDD
Akt
Glucose uptake
Cdk1

ABSTRACT

Insulin secretion and glucose transport are the major mechanisms to balance glucose homeostasis. Recently, we found that the death effector domain-containing DEDD inhibits cyclin-dependent kinase-1 (Cdk1) function, thereby preventing Cdk1-dependent inhibitory phosphorylation of S6 kinase-1 (S6K1), downstream of phosphatidylinositol 3-kinase (PI3K), which overall results in maintenance of S6K1 activity. Here we newly show that DEDD forms a complex with Akt and heat-shock protein 90 (Hsp90), and supports the stability of both proteins. Hence, in DEDD$^{-/-}$ mice, Akt protein levels are diminished in skeletal muscles and adipose tissues, which interferes with the translocation of glucose-transporter 4 (GLUT4) upon insulin stimulation, leading to inefficient incorporation of glucose in these organs. Interestingly, as for the activation of S6K1, suppression of Cdk1 is involved in the stabilization of Akt protein by DEDD, since diminishment of Cdk1 in DEDD$^{-/-}$ cells via siRNA expression or treatment with a Cdk1-inhibitor, increases both Akt and Hsp90 protein levels. Such multifaceted involvement of DEDD in glucose homeostasis by supporting both insulin secretion (via maintenance of S6K1 activity) and glucose uptake (via stabilizing Akt protein), may suggest an association of DEDD-deficiency with the pathogenesis of type 2 diabetes mellitus.

Introduction

The signalling cascade involving mitogen-related phosphatidylinositol 3-kinase (PI3K), Akt and their downstream TOR (target of rapamycin) is the central pathway that maintains glucose homeostasis in the body [1–4]. In mammals, upon stimulation by growth factors including insulin, the mammalian TOR (mTOR) cooperates with PI3K-dependent effectors to activate p70 ribosomal protein S6 kinase-1 (S6K1), thereby phosphorylating the 40S-ribosomal protein S6, and subsequently enhances translation of the 5′-terminal oligopyrimidine (5′-TOP) sequences that encode components of the translational machinery. This reaction increases the number of ribosomes and the efficacy of protein synthesis, thus critically promoting growth of types of cells including insulin-producing β cells within the pancreatic Langerhans islet [5–8]. The insulin mass was diminished in S6K1-deficient (S6K1$^{-/-}$) mice, resulting in ineffective secretion of insulin upon glucose administration [9]. Thus, S6K1 is involved in the machinery controlling glucose tolerance by supporting the size of β cells [10,11]. On the other hand, activation of Akt (in particular Akt2, the primary isoform in insulin-responsive tissues) induces translocation of glucose-transporter 4 (GLUT4) to the plasma membrane [12–15]. This response is responsible for glucose transport into cells. Thus, dysfunction of these elements provokes a phenotype similar to type 2 diabetes mellitus, which is a multifactorial disease with a variety of pathological defects in glucose homeostasis [16–18].

Recently, we defined the DEDD molecule as a critical element that maintains the activity of S6K1, thereby supporting the size of β cells and insulin mass in mice [19]. DEDD was initially described as a member of the death effector domain (DED)-containing protein family [20]. We previously found that DEDD is associated with the Cdk1/cyclin B1 complex, and that it decreases the kinase activity of Cdk1 [21]. This response impedes the Cdk1-dependent mitotic program to shut off synthesis of ribosomal RNA (rRNA) and protein, and is consequently useful in gaining sufficient cell growth [21,22]. Interestingly, DEDD also associates with S6K1, and interferes with the Cdk1-dependent inhibitory phosphorylation of S6K1 at several serine/threonine (Ser/Thr)

Abbreviations: DEDD, death effector domain-containing DNA binding protein; Cdk1, cyclin-dependent kinase-1; S6K1, S6 kinase-1; PI3K, phosphatidylinositol 3-kinase; rRNA, ribosomal RNA; TOR, target of rapamycin; mTOR, mammalian TOR; 5′-TOP, 5′-terminal oligopyrimidine; Thr, threonine; Ser, serine; MEF, mouse embryonic fibroblast; PDK1, phosphoinositide-dependent protein kinase-1; Hsp90, heat-shock protein 90; GLUT4, glucose-transporter 4.

* Corresponding author. Fax: +81 3 5841 1438.
E-mail address: tm@m.u-tokyo.ac.jp (T. Miyazaki).
[1] Present address: Department of Molecular Anatomy, Hamamatsu University School of Medicine, Hamamatsu, Shizuoka 431-3192, Japan.

0006-291X/$ - see front matter © 2009 Elsevier Inc. All rights reserved.
doi:10.1016/j.bbrc.2009.12.137

residues, including Ser411 and Ser424 sites within the auto-inhibitory tail [19,23,24]. This response maintains the activity of S6K1 preserving a high level of phosphorylation at Thr389, a hallmark of active S6K1 [19]. Hence in DEDD$^{-/-}$ mice, the activity of S6K1 was reduced in various cell types, and as observed in S6K1$^{-/-}$ mice, the insulin mass within pancreatic islets is reduced, resulting in overt glucose intolerance [19].

Having discovered the functional association of DEDD with S6K1, we here address a possible interaction of DEDD with Akt, and investigate a novel involvement of DEDD in the regulation of the insulin signaling cascade.

Material and methods

Mice. DEDD$^{-/-}$ mice [21] had been backcrossed to C57BL/6 (B6) for 17 generations before used for experiments. Mice are maintained under a SPF condition.

Antibodies. Antibodies used are: anti-total Akt (clone 11E7), anti-Akt phosphorylated at Thr308 (clone 244F9) (all are from Cell Signaling Technology, Beverly, MA); anti-Hsp90 (clone SPA-830) and anti-Cdk1 (clone A17) (from Stressgen, Victoria, BC, Canada, and Zymed Laboratories Inc., South San Francisco, CA).

Glucose incorporation. This assay was performed as described previously [25] with some modifications. Pieces from epididymal white fat pads and the soleus muscles of the mice were used. To determine 2-DG uptake, the muscles and fat pads were transferred to buffer A containing 1 mM 2-DG (0.5 μCi/ml 2-deoxy-D-[1-^{14}C]glucose) and 1 mM L-glucose (5 μCi/ml L-[1-^{3}H]glucose) with or without 10 nM insulin and incubated at 30 °C for 10 min. After the reaction is terminated, the samples were neutralized with 5 N HCl and dissolved in ACSII (Amersham Biosciences). ^{14}C and ^{3}H specific activities were counted by a liquid scintillation counter (Packard Instrument Co.).

GLUT4 translocation. Primary MEF cells prepared from DEDD$^{+/+}$ or DEDD$^{-/-}$ embryos were differentiated to adipocytes according to established protocols [26]. GLUT4 translocation assay was performed as previously described [26,27], using a GFP-fused GLUT4 expression vector [27]. Confluent primary MEF cells prepared from DEDD$^{+/+}$ or DEDD$^{-/-}$ mice were induced to differentiate by incubating the cells with DMEM containing 10 μg/ml of insulin (Sigma), 1 μM of dexamethasone (Sigma), and 500 μM of isobutylmethylxanthine (Sigma). After 48 h, the cells were fed with DMEM containing 10 μg/ml of insulin every 2 days prior to use. On 8–10 days after induction of differentiation, cells were transfected with the construction cording GFP-GLUT4-myc [27]. Cells were serum-starved for 4 hours, and then incubated with or without 200nM of insulin for 30 min. GFP-GLUT4 trafficking was followed by a fluorescent microscope. A ratio for GFP-GLUT4 distribution within peri-membrane areas to peri-nuclear areas was measured using NIH-Image.

Na_3VO_4 treatment. DEDD$^{+/+}$ or DEDD$^{-/-}$ MEF cells were enriched in metaphase by a treatment with 500 nM nocodazole (Sigma) for 24 h. Cells were further incubated with 10 mM Na_3VO_4 for an additional 6 h, and lysed in SDS sample buffer. The cell extracts were subjected to Western blotting using anti-Akt or anti-Hsp90 antibodies.

Protein degradation and phosphorylation assay. Subconfluent DEDD$^{+/+}$ or DEDD$^{-/-}$ MEF cells were cultured accordingly and harvested at indicated time points after treatment with 100 μg/ml cyclohexamide with or without 10 μM MG-132 and 0.4 mM chloroquine, lysed with Briji 97 lysis buffer supplemented with 5 mM iodoacetamide, 5 μg/ml leupeptin, 0.2 mM AEBSF, 1 mM Na_3VO_4, and 10 mM NaF. Lysates were resolved onto SDS–PAGE, and immunoblotted anti-Akt antibody.

siRNA transfection. Double strands siRNA targeting DEDD or Cdk1 were purchased from Applied Biosystems or SIGMA, respectively. Wild-type MEF cells at 50% confluency were transfected with 10 μM siRNA using Lipofectamine 2000 (Invitrogen Inc.). Forty-eight hours after the transfection, the cells were harvested and analyzed by Western blotting or RT-PCR. Sequences of the oligonucleotides were as follows: DEDD siRNA#1: 5′-GCCCTGATC TTGTAGACAATT-3′, DEDD siRNA#2: 5′-AAATGGACGTGACTTCTTA TT-3′, Cdk1 siRNA#1: 5′-CTATGATCCTGCCAAACGATT-3′, Cdk1 siRNA#2: 5′-GTTGTTTACCGTTGGCTCTTT-3′, Cdk1 siRNA#3: 5′-CAATC AAACTGGCTGATTTTT-3′. For a control, an oligonucleotide targeting GFP sequence (Sigma) was used.

Primers for RT-PCR. Primers used are as follows: for, forward primer; rev, reverse primer. Hsp90α for: 5′-GCGGCAAAGACAAGAAA AAG-3′; Hsp90α rev: 5′-CAAGTGGTCCTCCCAGTCAT-3′; Hsp90β for: 5′-CTGGGTCAAGCAGAAAGGAG-3′; Hsp90β rev: 5′-TCTCTGTTG CTTCCCGACTT-3′; Akt1 for: 5′-CCACGCTACTTCCTCCTC-3′; Akt1 rev: 5′-TGCCCTTGCCAACAGTCTGAAGCA-3′; Akt2 for: 5′-GTCGCC AACAGTCTGAAGCA-3′; Akt2 rev: 5′-GAGAGAGGTGGAAAAACAG C-3′; G3PDH for: 5′-ACCACAGTCCATGCCATCAC-3′; G3PDH rev: 5′-TCCACCACCCTGTTGCTGTA-3′; β-actin for: 5′-GTGGCTACAGCTTC ACCACCACAG-3′; β-actin rev: 5′-GCATCCTGTCAGCAATGCCTGGG T-3′; DEDD for: 5′-GCGGGATCCGCGGGCCTAAAGAGGC-3′; DEDD rev: 5′-GCGTCTAGAGTCTACAAGATCAGGGC-3′.

Quantification of immuno-blots. Quantification of the immunoblots was performed using the NIH-Image. Relative phosphorylation levels to those in control (shown as 1.0 ± SEM) are presented. For all immuno-blotting experiments, at least three independent blotting were performed.

Statistical analysis. A two-tailed Mann–Whitney test was used to calculate *P*-values. (**): $P < 0.01$, (*): $P < 0.05$. Error bars: SEM.

Results

Lack of DEDD decreases the amount of Akt protein

Having observed reduced activity of S6K1 in the absence of DEDD [19], we wondered whether upstream of S6K1 in the insulin signalling pathway might also be influenced by the lack of DEDD, and thus assessed the situation of Akt protein in DEDD$^{-/-}$ mouse embryonic fibroblast (MEF) cells by Western blotting. To our surprise, the amount of Akt was also greatly decreased in DEDD$^{-/-}$ MEF cells compared with DEDD$^{+/+}$ MEF cells, when tested by using an antibody that detects all isotypes of Akt (Fig. 1A, total Akt). Signals for activated Akt phosphorylated at Thr308 residue were also reduced, along with the diminished amounts of total Akt protein (Fig. 1A, p-Akt). A reduction in the amount of Akt as well as in the Thr308 phosphorylation level, was also clear in DEDD$^{-/-}$ skeletal muscles and adipose tissues, where Akt plays an important role in the regulation of glucose homeostasis [12,13] (Fig. 1B). The effect of an acute loss of DEDD on Akt was also assessed by knocking down DEDD in cells. As presented in Fig. 1C, downregulation of DEDD expression by introducing a double-stranded siRNA for DEDD into wild-type MEF cells significantly reduced the amount of Akt. Consistent with these observations, the activating phosphorylation (at Ser2448) of mTOR, downstream of Akt, was decreased in DEDD$^{-/-}$ compared with DEDD$^{+/+}$ cells (Fig. 1D, left). In contrast, phosphorylation levels of 3-phosphoinositide-dependent protein kinase-1 (PDK1), which phosphorylates Akt, were comparable in the presence or absence of DEDD, suggesting that the less phosphorylation of Akt in the absence of DEDD is mainly caused by a reduction in the total amount of Akt protein (Fig. 1E). Together, the lack of DEDD decreases the amount of all types of Akt protein both in MEF cells and in tissues from DEDD$^{-/-}$ mice, which is accompanied with lower Akt activity. This

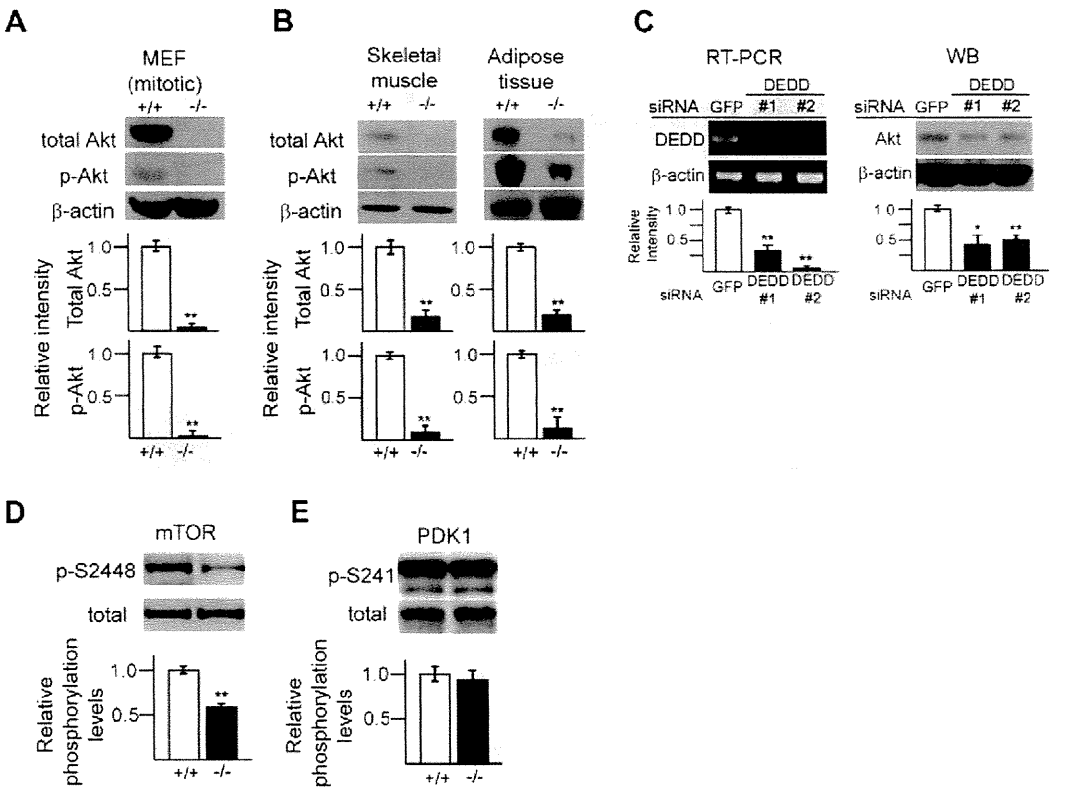

Fig. 1. Reduced Akt protein amounts in the absence of DEDD. (A) Total Akt or phosphorylated (activated) Akt analyzed in DEDD$^{+/+}$ and DEDD$^{-/-}$ MEF cells, and (B) in tissues from DEDD$^{+/+}$ and DEDD$^{-/-}$ mice. The representative immuno-blots and the averages of relative intensities (+/+ as 1.0) from all experiments are presented. Error bar: SEM. (C) Increase of Akt levels by diminishment of DEDD using siRNA in DEDD$^{-/-}$ MEF cells. DEDD mRNA and Akt protein levels relative to those in control (shown as 1.0) are also presented. (D) Activative phosphorylation of mTOR (at Ser2448 site) and (E) PDK1 (at Ser241 site) in DEDD$^{+/+}$ or DEDD$^{-/-}$ MEF cells was analyzed by Western blotting. For PDK1, two bands appear when this polyclonal antibody (Cell signalling; #3061) is used as described in its data sheet provided from the company. The upper band is the phosphorylated PDK1. Three independent experiments (for both D and E) were performed.

result also indicates that in the absence of DEDD, the reduction in Akt activity may partly be responsible for the decreased S6K1 activity, in addition to the increased phosphorylation levels at the inhibitory residues of S6K1 brought about by the hyper activity of Cdk1 [19].

DEDD forms a complex with Akt and Hsp90, and stabilizes these proteins

Although the amount of Akt protein is markedly reduced, mRNA for both Akt1 and Akt2 were expressed at similar levels in DEDD$^{-/-}$ and DEDD$^{-/-}$ tissues and cells (Fig. 2A). This result suggests that DEDD may be necessary for the maintenance of Akt protein. To test this possibility, we measured the half-life of Akt protein in DEDD$^{-/-}$ and DEDD$^{+/+}$ MEF cells. Importantly, the amount of Akt protein was decreased in 10 hours in DEDD$^{-/-}$ cells, but not in DEDD$^{+/+}$ cells (Fig. 2B). The presence of MG-132, a proteasome inhibitor, tempered the reduction observed in DEDD$^{-/-}$ cells (Fig. 2B). Thus, the lack of DEDD results in instability of Akt protein.

Several groups reported that heat-shock protein 90 (Hsp90), a chaperone required for the conformational maturation of certain signalling proteins, forms a complex with Akt and is involved in its stabilization [28,29]. Thus, we assessed the protein levels of Hsp90 in DEDD$^{+/+}$ and DEDD$^{-/-}$ MEF and tissues. As depicted in Fig. 2C, the amount of Hsp90 protein also decreased in skeletal muscle, adipose tissue, as well as in MEF cells from DEDD$^{-/-}$ mice compared with those from DEDD$^{+/+}$ mice, whereas the transcripts of *Hsp90* (both α and β) genes were at an equivalent level in both types of mice (Fig. 2D). Furthermore, as depicted in Fig. 2E, immunoprecipitation assays revealed that DEDD associates with Akt (both 1 and 2) and Hsp90. Together, DEDD appears to facilitate a stable complex with Akt and Hsp90, supporting the levels of these proteins.

Suppression of Cdk1 increases Akt protein levels in DEDD$^{-/-}$ cells

As we demonstrated in a previous report, DEDD modulates the activity of S6K1 partly via suppressing Cdk1 activity [19]. To assess whether the inhibitory effect of DEDD on Cdk1 is also involved in stabilizing Akt protein, we knocked down Cdk1 in DEDD$^{-/-}$ MEF cells by introducing double-stranded siRNA for Cdk1, and analyzed the Akt and Hsp90 protein levels. As demonstrated in Fig. 3A, the levels of both proteins increased in DEDD$^{-/-}$ cells when Cdk1 protein was diminished. In addition, treatment of DEDD$^{-/-}$ MEF cells with sodium orthovanadate (VO_4), which is commonly used to inactivate Cdk1 [24], significantly increased the levels of both Akt and Hsp90 (Fig. 3B). These data suggest that in DEDD$^{-/-}$ cells, the increase in Cdk1 activity appeared to be responsible to the instability of Akt protein.

Attenuated glucose incorporation in DEDD$^{-/-}$ skeletal muscles and adipose tissues

One of a variety of functions for Akt is the regulation of incorporation of glucose into cells in response to insulin [30–32]. It is well known that translocation of GLUT4 to the plasma membrane upon insulin stimulation is a key mechanism of glucose transport into cells [12,13], and that this translocation of GLUT4 is dependent on activation of Akt, in particular Akt2 [33–35]. Therefore, we assessed how the reduction of the amount of Akt caused by the ab-

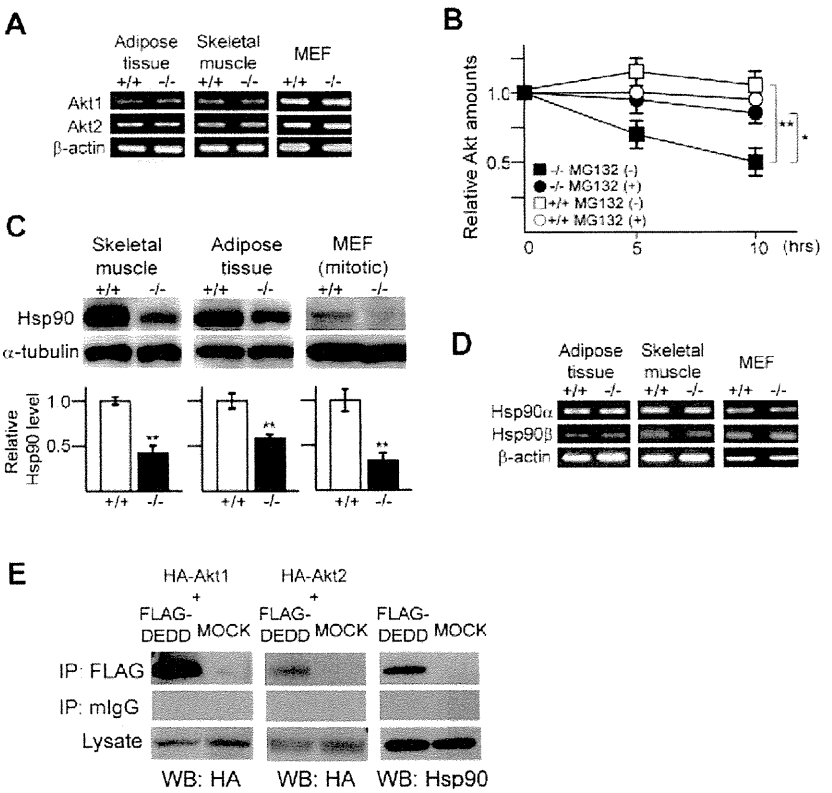

Fig. 2. DEDD forms a complex with Akt and Hsp90 and supports the stability of these proteins. (A) RT-PCR for Akt1, Akt2, and β-actin as a control (performed within the linear range). (B) Protein degradation assay for Akt. Representative data out of comparable results obtained by two independent experiments is presented. (C) Hsp90 protein levels in DEDD$^{+/+}$ or DEDD$^{-/-}$ skeletal muscle, adipose tissue or mitotic MEF cells. (D) RT-PCR assay for Hsp90 mRNA. (E) Association of DEDD with Akt1, Akt2, and Hsp90. DEDD was precipitated from 293T cells expressing HA-tagged AKt1 or Akt2 with or without FLAG-DEDD, and the precipitates were analyzed for HA-Akt1 or 2 using an anti-HA antibody (left and middle). Likewise, endogenous Hsp90 was co-precipitated with FLAG-DEDD from 293T cells expressing FLAG-DEDD (right). Results from the control IP using a mouse-IgG (mIgG) are also demonstrated.

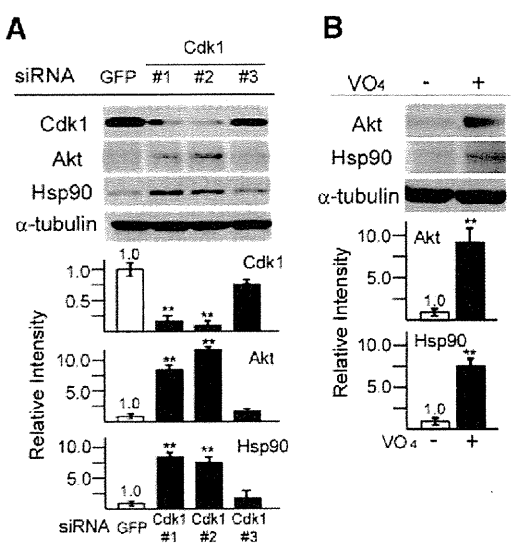

Fig. 3. Involvement of Cdk1 in stabilization of Akt by DEDD. (A) Akt and Hsp90 levels in mitotic DEDD$^{-/-}$ MEF cells after treatment with siRNA targeting Cdk1 (three distinct sequences), or (B) with Na_3VO_4 (VO_4) for 6 h. The levels of Akt and Hsp90 relative to those in control (shown as 1.0) are also presented.

sence of DEDD affects glucose uptake in mice. As shown in Fig. 4A, the uptake of glucose by skeletal muscle (soleus muscles) and adipose tissue in response to insulin was significantly damaged in DEDD$^{-/-}$ mice. We also tested GLUT4 translocation in response to insulin, using DEDD$^{-/-}$ and DEDD$^{+/-}$ adipocytes differentiated from MEF cells. The increase of GLUT4 on the cell membrane after an insulin challenge was significantly less in DEDD$^{-/-}$ compared to DEDD$^{+/+}$ cells (Fig. 4B). Hence, diminished levels of Akt correlated with inefficient induction of GLUT4 translocation, resulting in deficient glucose transport into cells in DEDD$^{-/-}$ skeletal muscle and adipose tissue.

Interestingly, however, Akt levels were almost comparable in the liver in DEDD$^{-/-}$ and DEDD$^{+/+}$ mice, in contrast to levels in skeletal muscle and adipose tissue (Fig. 4C). As the endogenous DEDD expression level was lower in the liver compared with that in the skeletal muscle (Fig. 4D), the loss of DEDD might not strongly influence Akt stability in the liver as it did in the skeletal muscle or adipose tissue.

Discussion

In addition to our previous report in which DEDD maintains the activity of S6K1 supporting the insulin mass within pancreatic islets, our current study has demonstrated that DEDD stabilizes Akt protein, leading to efficient glucose transport into skeletal muscles and adipose tissues. Thus, DEDD is involved in the insulin signalling pathway at diverse levels (summarized in Fig. 4E). As type 2 diabetes mellitus is a multifactorial disease [17], our findings suggest that DEDD-deficiency might play a certain role in the pathology of type 2 diabetes mellitus. Indeed, the defect in glucose transport observed in DEDD$^{-/-}$ mice is one of the essential pathogenic features in type 2 diabetes mellitus. Evidence has also

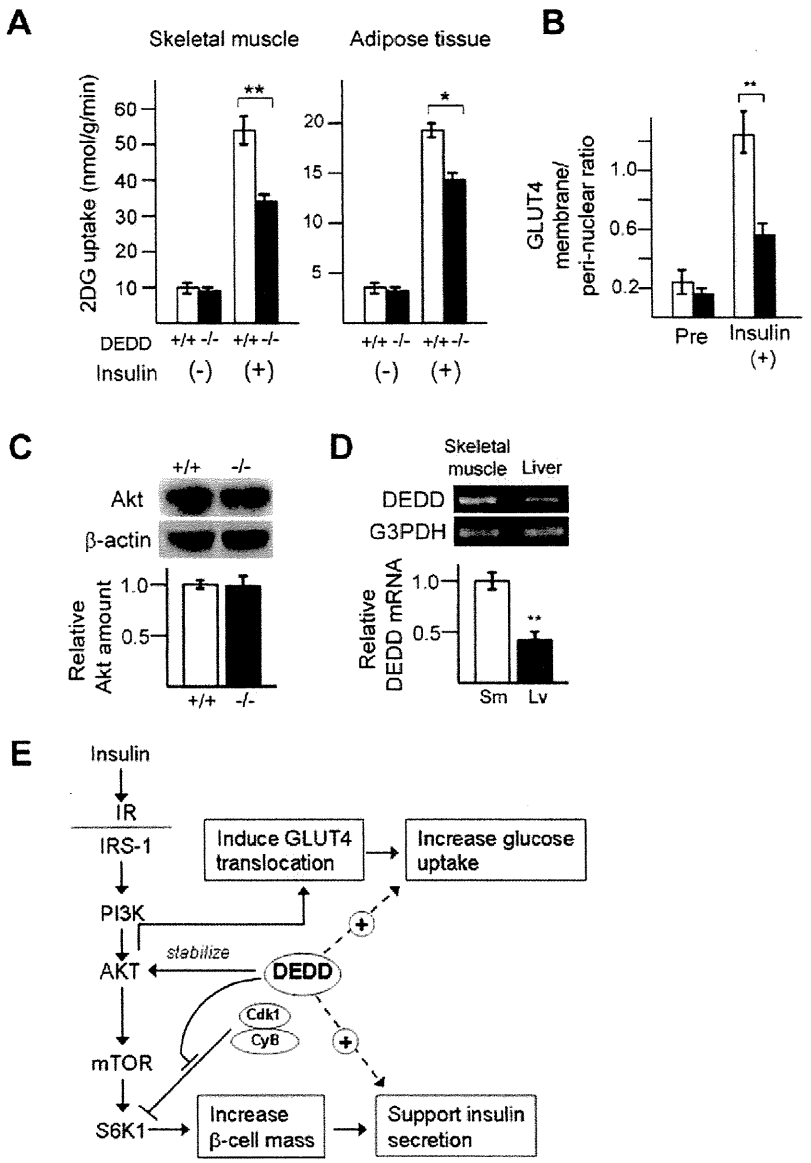

Fig. 4. Defects in glucose incorporation in DEDD$^{-/-}$ tissues. (A) Glucose incorporation by skeletal muscle (left) or adipose tissue (right) ($n = 5$ each). (B) Translocation of GLUT4 in DEDD$^{+/+}$ (white bars) or DEDD$^{-/-}$ (black bars) adipocytes. Data represent the relative amount of GFP-GLUT4 at the membrane locus to that at the peri-nuclear area. Data are the averages of results from 30 cells. (C) Akt protein levels in DEDD$^{-/-}$ and DEDD$^{+/+}$ liver. (D) DEDD mRNA level expressed in the liver (Lv) relative to that in the skeletal muscle (Sm) is presented (lower panel). (E) A scheme for the plausible involvement of DEDD in glucose homeostasis. IR, insulin receptor; CyB, cyclin B1. The + with a dashed line (that starts from DEDD) means positive effect.

shown that a decrease in insulin secretion and reduced β cell mass do contribute to development of the disease [16,18].

It is interesting that the decrease in Akt protein levels was variable in different DEDD$^{-/-}$ tissues important for glucose homeostasis; i.e. it was prominent in the skeletal muscles and adipose tissues, but was not very significant in the liver. This might cause a variable aberrancy in glucose transport in different organs in DEDD$^{-/-}$ mice. Additional experiments such as to test the insulin sensitivity in each tissue, will test this possibility. It may be noteworthy that such a variation in insulin sensitivity in different tissues is often seen in human patients [16–18]. It will also be important to address whether any dysfunction of DEDD is present, either in the whole body or in specific tissues, in a subset of type 2 diabetes patients.

The precise mechanism of how the association of DEDD with Akt and Hsp90 supports the stability of these proteins is still unclear. The DEDD's effect on Akt stability appears to be achieved through Cdk1. As we previously demonstrated, increased Cdk1 activity in the absence of DEDD accelerates the phosphorylation levels at the inhibitory residues of S6K1, resulting in a reduction of S6K1 activity [19]. A similar scenario might also be true for Akt (and/or Hsp90), although so far, inhibitory phosphorylation sites are not known either in Akt or Hsp90. Otherwise, Cdk1 might phosphorylate and activate some ubiquitin ligase(s) that degenerate Akt. As reviewed by Hunter [36], multiple crosstalks between phosphorylation and ubiquitination occur differentially during the protein degradation. Phosphorylation can regulate ubiquitination of a protein in different manners. Firstly, phosphorylation positively or negatively regulates the activity of the E3 ligase responsible for ubiquitine transfer. It is possible that Cdk1 may phosphorylate some E3 ligase(s) responsible for ubiquitination and degradation of Akt. Indeed, some E3 ligases involved in degradation of Akt, including recently identified TTC3 [37], require phosphorylation for their activation. Whilst, activity of CHIP, a major E3

ligase responsible for ubiquitination of Akt [38,39], might be modified directly or indirectly by Cdk1-depedent phosphorylative events, though the direct phosphorylation of CHIP has not been reported. On the other hand, it is also known that phosphorylation also promotes recognition of substrates by an E3 ligase [40]. However, phosphorylation events of Akt promoted by Cdk1 have not yet demonstrated. Alternatively, the possibility that formation of DEDD/Akt/Hsp90 might structurally stabilize these participant proteins is not mutually excluded. Thus, the molecular linkage among DEDD, Cdk1 and Akt-degradation still remains to be further addressed.

Conclusions

In summary, we newly demonstrated that DEDD plays an important role in maintenance of the Akt protein level, which in consequence supports the efficient incorporation of glucose into skeletal muscles and adipose tissues. Further investigations might find an unknown relevance of DEDD to the insulin signalling pathway, and thus, with a novel pathogenesis of type 2 diabetes mellitus.

Acknowledgments

We thank to Drs. T. Kubota, T. Kadowaki, T. Ide, K. Murakami, F. Suizu, M. Noguchi for technical assistance and useful discussion; Drs. S. Nishimura and M.P. Czech for the GFP-GLUT4 vector. This work was supported by Grants-in-Aid for Scientific Research (B) (Japan Society for the Promotion of Science), NIH (5RO1AI50948), Research Fund of Mitsukoshi Health and Welfare Foundation, Mitsubishi Pharma Research Foundation, (to T.M.), Kanae Foundation for the Promotion of Medical Science, Astellas Foundation for Research on Metabolic Disorders, and Ono Medical Research Foundation (to S.A.).

References

[1] E. Jacinto, M.N. Hall, Tor signalling in bugs, brain and brawn, Nat. Rev. Mol. Cell. Biol. 4 (2003) 117–126.
[2] S. Oldham, E. Hafen, Insulin/IGF and target of rapamycin signaling: a TOR de force in growth control, Trends Cell Biol. 13 (2003) 79–85.
[3] B. Valentinis, R. Baserga, IGF-I receptor signalling in transformation and differentiation, Mol. Pathol. 54 (2001) 133–137.
[4] P.K. Vogt, PI 3-kinase, mTOR, protein synthesis and cancer, Trends Mol. Med. 7 (2001) 482–484.
[5] D.C. Fingar, J. Blenis, Target of rapamycin (TOR): an integrator of nutrient and growth factor signals and coordinator of cell growth and cell cycle progression, Oncogene 23 (2004) 3151–3171.
[6] S. Huang, P.J. Houghton, Targeting mTOR signaling for cancer therapy, Curr. Opin. Pharmacol. 3 (2003) 371–377.
[7] F. Shamji, P. Nghiem, S.L. Schreiber, Integration of growth factor and nutrient signaling: implications for cancer biology, Mol. Cell 12 (2003) 271–280.
[8] Vivanco, C.L. Sawyers, The phosphatidylinositol 3-kinase AKT pathway in human cancer, Nat. Rev. Cancer 2 (2002) 489–501.
[9] M. Pende, S.C. Kozma, M. Jaquet, et al., Hypoinsulinaemia, glucose intolerance and diminished beta-cell size in S6K1-deficient mice, Nature 408 (2000) 994–997.
[10] S.G. Dann, A. Selvaraj, G. Thomas, mTOR complex1–S6K1 signaling: at the crossroads of obesity, diabetes and cancer, Trends Mol. Med. 13 (2007) 252–259.
[11] S.H. Um, D. D'Alessio, G. Thomas, Nutrient overload, insulin resistance, and ribosomal protein S6 kinase 1, S6K1, Cell Metab. 3 (2006) 393–402.
[12] M.M. Hill, S.F. Clark, D.F. Tucker, et al., A role for protein kinase Bbeta/Akt2 in insulin-stimulated GLUT4 translocation in adipocytes, Mol. Cell. Biol. 19 (1999) 7771–7781.
[13] S. Huang, M.P. Czech, The GLUT4 glucose transporter, Cell Metab. 5 (2007) 237–252.
[14] S.A. Summers, L.A. Garza, H. Zhou, M.J. Birnbaum, Regulation of insulin-stimulated glucose transporter GLUT4 translocation and Akt kinase activity by ceramide, Mol. Cell. Biol. 18 (1998) 5457–5464.
[15] E.L. Whiteman, H. Cho, M.J. Birnbaum, Role of Akt/protein kinase B in metabolism, Trends Endocrinol. Metab. 13 (2002) 444–451.
[16] G.I. Bell, K.S. Polonsky, Diabetes mellitus and genetically programmed defects in beta-cell function, Nature 414 (2001) 788–791.
[17] R.A. DeFronzo, Pathogenesis of type 2 diabetes: metabolic and molecular implications for identifying diabetes genes, Diabetes Rev. 5 (1997) 177.
[18] B.B. Kahn, L. Rossetti, Type 2 diabetes—who is conducting the orchestra?, Nat Genet. 20 (1998) 223–225.
[19] N. Kurabe, S. Arai, A. Nishijima, et al., The death effector domain-containing DEDD supports S6K1 activity via preventing Cdk1-dependent inhibitory phosphorylation, J. Biol. Chem. 284 (2009) 5050–5055.
[20] H. Stegh, O. Schickling, A. Ehret, et al., DEDD, a novel death effector domain-containing protein, targeted to the nucleolus, EMBO J. 17 (1998) 5974–5986.
[21] S. Arai, K. Miyake, R. Voit, et al., The death-effector domain containing protein DEDD is a novel mitotic inhibitor requisite for cell growth, Proc. Natl. Acad. Sci. USA 104 (2007) 2289–2294.
[22] T. Miyazaki, S. Arai, Two distinct controls of mitotic Cdk1/cyclin B1 requisite for cell growth prior to cell division, Cell Cycle 6 (2007) 1419–1425.
[23] P.J. Papst, H. Sugiyama, M. Nagasawa, et al., Cdc2-cyclin B phosphorylates p70 S6 kinase on Ser411 at mitosis, J. Biol. Chem. 273 (1998) 15077–15084.
[24] O.J. Shah, S. Ghosh, T. Hunter, J. Biol. Chem. 278 (2003) 16433–16442.
[25] N. Kamei, K. Tobe, R. Suzuki, et al., Overexpression of monocyte chemoattractant protein-1 in adipose tissues causes macrophage recruitment and insulin resistance, J. Biol. Chem. 281 (2006) 26602–26614.
[26] S. Bogan, A.E. McKee, H.F. Lodish, Insulin-responsive compartments containing GLUT4 in 3T3-L1 and CHO cells: regulation by amino acid concentrations, Mol. Cell. Biol. 21 (2001) 4785–4806.
[27] Z.Y. Jiang, A. Chawla, A. Bose, et al., A phosphatidylinositol 3-kinase-independent insulin signaling pathway to N-WASP/Arp2/3/F-actin required for GLUT4 glucose transporter recycling, J. Biol. Chem. 277 (2002) 509–515.
[28] D. Basso, D.B. Solit, G. Chiosis, et al., Akt forms an intracellular complex with heat shock protein 90 (Hsp90) and Cdc37 and is destabilized by inhibitors of Hsp90 function, J. Biol. Chem. 277 (2002) 39858–39866.
[29] D.B. Solit, A.D. Basso, A.B. Olshen, et al., Inhibition of heat shock protein 90 function down-regulates Akt kinase and sensitizes tumors to Taxol, Cancer Res. 63 (2003) 2139–2144.
[30] D.P. Brazil, Z.Z. Yang, B.A. Hemmings, Advances in protein kinase B signalling: AKTion on multiple fronts, Trends Biochem. Sci. 29 (2004) 233–242.
[31] B.D. Manning, L.C. Cantley, AKT/PKB signaling: navigating downstream, Cell 129 (2007) 1261–1274.
[32] K. Du, P.N. Tsichlis, Regulation of the Akt kinase by interacting proteins, Oncogene 24 (2005) 7401–7409.
[33] H. Cho, J. Mu, J.K. Kim, J.L. Thorvaldsen, et al., Insulin resistance and a diabetes mellitus-like syndrome in mice lacking the protein kinase Akt2 (PKB beta), Science 292 (2001) 1728–1731.
[34] R.S. Garofalo, S.J. Orena, K. Rafidi, et al., Severe diabetes, age-dependent loss of adipose tissue, and mild growth deficiency in mice lacking Akt2/PKB beta, J. Clin. Invest. 112 (2003) 197–208.
[35] Y. Ng, G. Ramm, J.A. Lopez, D.E. James, Rapid activation of Akt2 is sufficient to stimulate GLUT4 translocation in 3T3-L1 adipocytes, Cell Metab. 7 (2008) 348–356.
[36] T. Hunter, The age of crosstalk: phosphorylation, ubiquitination, and beyond, Mol. Cell 28 (2007) 730–738.
[37] F. Suizu, Y. Hiramuki, F. Okumura, et al., The E3 ligase TTC3 facilitates ubiquitination and degradation of phosphorylated Akt, Dev. Cell 17 (2009) 800–810.
[38] C.A. Dickey, J. Koren, Y. Zhang, et al., Akt and CHIP coregulate tau degradation through coordinated interactions, Proc. Natl. Acad. Sci. USA 105 (2008) 3622–3627.
[39] V. Facchinetti, W. Ouyang, H. Wei, et al., The mammalian target of rapamycin complex 2 controls folding and stability of Akt and protein kinase C, EMBO J. 27 (2008) 1932–1943.
[40] T. Xiang, A. Ohashi, Y. Huang, et al., Negative Regulation of AKT Activation by BRCA, Cancer Res. 168 (2008) 10040–10044.